5. Results and Discussion

5.1. HPLC analytical method development

Standard calibration curve of BBR was linear over the range 2 - 10 µg/ml and the retention of BBR was 8 min. The regression equation was y = 23.044 x – 0.9048 and mean correlation coefficient (R^2) was 0.9999. The accuracy (% of recovery) values of 2, 5 and 10 µg/ml were 80.3%, 87.6% and 88.4%, respectively. The coefficients of variation (CV) for intra and inter day precision were less than 10%, and the LOQ was 0.55 µg/ml, and LOD was 0.105 µg/ml. The validation parameters are mentioned in Table 5.1. Calibration curve obtained from the HPLC analysis and a representative chromatogram of BBR is shown in Figure 5.1. and 5.2.

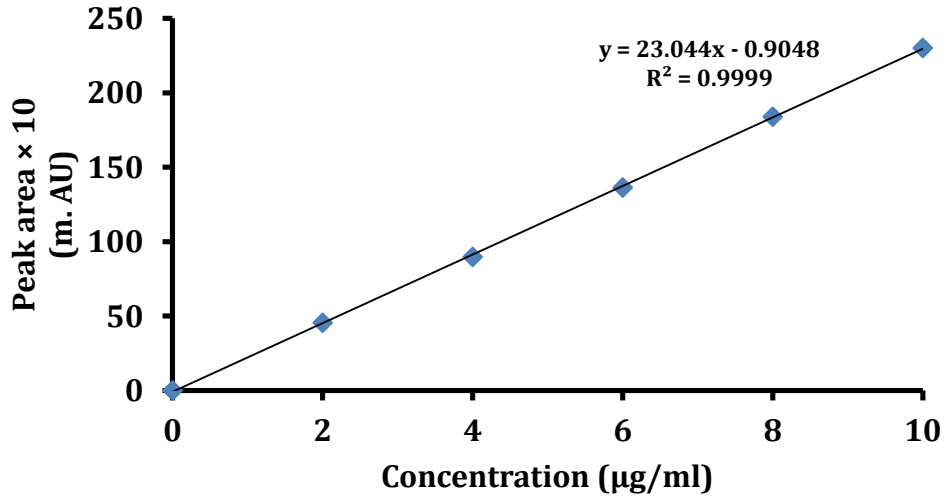

Figure 5.1. Standard curve of Berberine

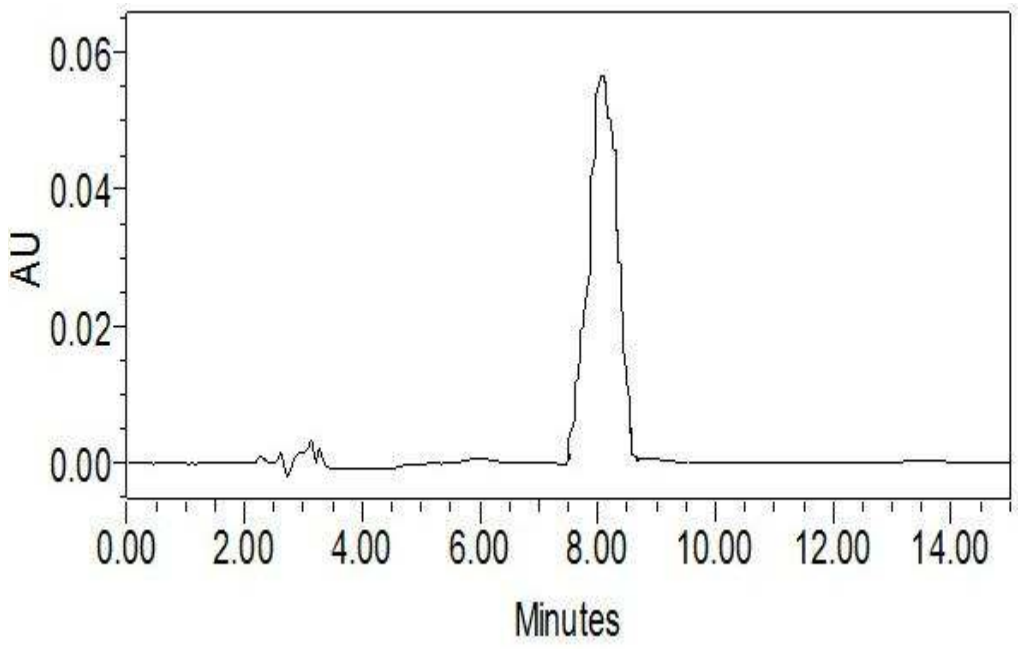

Figure 5.2. HPLC chromatogram of Berberine

Table 5.1. HPLC analytical method validation parameters

Parameters		**Results**
Range		2 -10 µg/ml
Regression equation		y = 23.044.x-0.9098
Regression coefficient (R^2)		0.999
Accuracy (% Recovery)		95 ± 2.45
Precision (%CV)	Intra-Day	1.13 ± 0.62
	Inter-Day	1.87 ± 0.91
LOD (µg/ml)		0.105
LOQ (µg/ml)		0.550

5.2. Solubility study in aqueous, different pH solutions and surfactants

BBR exhibited pH independent solubility at 25°C and the results are shown in Figure 5.3. and Table 5.2. The aqueous solubility of BBR found to be 3.257 ± 0.8 mM. The solubility of BBR 3.984 ± 0.42 mM and 4.127 ± 0.27 mM in pH 6.8 and 7.2 phosphate buffers, respectively which was significantly higher than the solubility in water. The lowest solubility (0.956 ± 0.29 mM) was found at pH 4.5 phthalate buffer. In nanoprecipitation technique, entrapment of hydrophobic drugs is not affected by the used aqueous phase because of low solubility of drug in aqueous phase. In case of hydrophilic drugs, the poor entrapment in nanoparticles was observed with aqueous phase. The drug being soluble in the aqueous phase is not available for entrapment in to the polymer during preparation of nanoparticles and this leads to poor entrapment in nanoparticles. To overcome this problem, the aqueous phase with limited capacity to solubilize the drug is selected. This reduces the solubility and subsequently improves the availability of drug for entrapment into the polymeric nanoparticle. Thus, on the basis of results of solubility studies, pH 4.5 phthalate buffer was selected as a aqueous phase for preparation of BBR loaded nanoparticles. It is expected that the lowest solubility of BBR in selected aqueous phase (pH 4.5 phthalate buffers) can provide

higher amount of BBR in organic phase during the process and may lead to improvement in entrapment of BBR in nanoparticles.

Surfactants are used as stabilizers in order to avoid the aggregation of generated nanoparticles during the preparation and at storage. Apart from the intended function, surface tension reduction property of surfactants considerably increases solubility of the drug in aqueous phase and promotes the moving of drug from organic phase to aqueous phase. Ultimately, it hampers the attaining of higher entrapment of hydrophilic drug into nanoparticles. Therefore, selection of the proper stabilizer is an important aspect in the preparation of nanoparticles which does not enhance the solubility of hydrophilic drugs in aqueous phase and consequently facilitates higher entrapment.

For this purpose solubility studies were conducted on BBR with commonly used ionic and non ionic surfactants at different concentrations in pH 4.5 phthalate buffer which was selected as an aqueous phase. The results are shown in Figure 5.4. and Table 5.3. There was no significant change ($p < 0.05$) in solubility of BBR at pH 4.5 phthalate buffers in presence of F-68 and T-80 (non–ionic) surfactants in the range of 10 – 50 mM. The inadequate formation of micelles in pH 4.5 and low intermolecular interaction between positive charged drug and non ionic surfactants may be probable reason behind the insignificant enhancement in the solubility of BBR. Similarly, no significant difference

in the solubility was observed when SLS (anionic) and CTAB (cationic) were used at 10 and 25 mM. However, insignificant reduction in the solubility of BBR with SLS and CTAB at 50 mM could be due to formation of insoluble complexes and charge based repulsiveness with surfactants (Battu *et al*., 2010). The results indicate that all of the above surfactants can be used as a stabilizer due to their insignificant effect on solubility of BBR. Finally, F – 68 was selected as a stabilizer due to its extensive compatible character and wide use in preparation of nanoparticles.

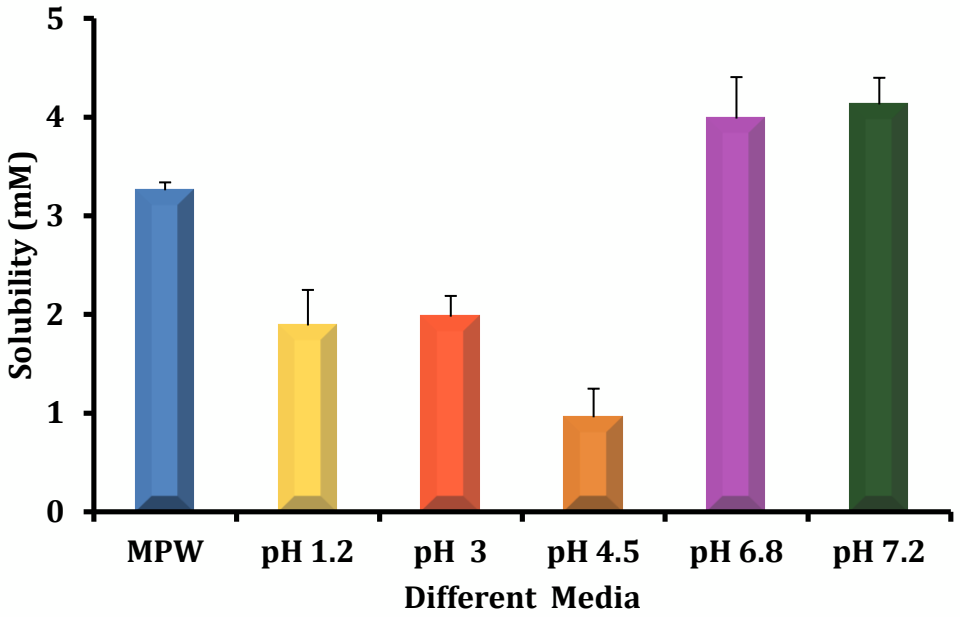

Figure 5.3. Solubility studies of BBR in different media

Table 5.2. Solubility studies of BBR in different media

Media	Solubility (mM)
MPW	3.257 ± 0.08
pH 1.2 (Hydrochloric acid buffer)	1.887 ± 0.36
pH 3.0 (Acid phthalate buffer)	1.976 ± 0.21
pH 4.5 (Neutralized phthalate buffer)	0.956 ± 0.29
pH 6.8 (Phosphate buffer)	3.984 ± 0.42
pH 7.2 (phosphate buffer)	4.127 ± 0.27

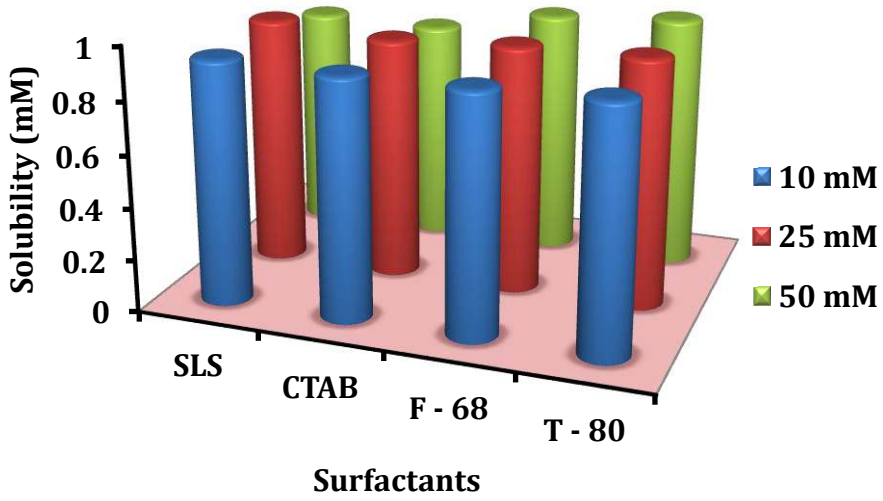

Figure 5.4. Solubility studies of BBR in different surfactants in pH 4.5 buffer

Table 5.3. Solubility studies of BBR in different surfactants in pH 4.5 phthalate buffer

Surfactants Concentration (mM)	Solubility in different surfactants (mM)			
	SLS	CTAB	F - 68	T - 80
10	0.93± 0.03	0.919± 0.02	0.922± 0.03	0.936± 0.02
25	0.951± 0.02	0.92± 0.04	0.942± 0.04	0.947± 0.01
50	0.856± 0.04	0.848± 0.06	0.936± 0.02	0.962± 0.02

5.3. Development of Nanoformulations (BBR-NP and BBR-SCNP)

5.3.1. Optimization of process variables

Size of the needle (diameter), injection rate and stirring rate affected the mean particle size of the placebo nanoparticles. The results are shown in Table 5.4.

5.3.1.1. Effect of needle size

Significant difference in particles size was observed with increase in number of needle from 20 G (0.90 mm i.d) to 26 G (0.45 mm i.d) where as injection rate at 6ml/min with two different stirring rates (800 and 1200 rpm). No significant increase in particle size observed while increase in needle size at injection rate (12 ml/min) with two different stirring rates (800 and 1200 rpm). However, the smaller particle size (196.12 ± 03.37 nm) of batch 3 was observed with needle size 26 (0.45 mm i.d). It

indicates that smaller diameter of the needle produces smaller size of the particles.

5.3.1.2. Effect of injection rate

Increase in the rate of injection from 6 ml/min to 12 ml/min leads to increase in particle size was observed in all batches while other variables kept constant. For instance, lower particle size was observed with injection rate at 6 ml/min (batch 3) where as further increasing of injection rate (12 ml/min) lead to increase in particle size (batch 8). However, the batches 1 and 2 prepared at 6 ml/min produced larger particle size. It may be the effect of larger diameter of the needle size 20 G (0.90 mm i.d) and aggregation of particles at higher stirring rate (1200 rpm). Using a high injection rate caused phase separation as whole organic phase is introduced at once into the aqueous phase providing inadequate time for diffusion of organic solvent preventing nanoprecipitation and causing separation of polymer. It may cause particle aggregation and generation of larger size particles. The results suggests that injection rate at 6 ml/min is suitable for producing of smaller size particles.

5.3.1.3. Effect of stirring rate

The significant increase in the particle size observed with increase in the stirring rate from 800 rpm to 1200 rpm of batches 1 to 4. It may be due to the aggregation of nanoparticles at higher stirring rate due to vortex

formation. The vortex allows accumulation of organic phase leading to polymer- polymer interaction and phase separation. Further, the batches 5 to 8 showed insignificant difference in particle size while increasing the stirring rate. It indicates that injection rate have greater influence rather stirring rate and needle size. The results suggest that stirring rate at 600 rpm is enough for generation of nanoparticles.

Based on the above results, needle size number 26 G (0.45 mm i.d), Injection rate 6ml/min and stirring rate 800 rpm selected as optimized process variables and used for preparation of BBR loaded nanoparticles. These results reiterate the earlier findings (Singh and Muthu, 2007).

Table 5.4. Effect of Injection rate, needle size and stirring rate on particle size of placebo nanoparticles

Batch	Injection rate (ml/min)	Needle size (No)	Stirring rate (rpm)	Particle size (nm)
1	6	20	800	495.31 ± 08.67
2	6	20	1200	608.71 ± 32.4
3	6	26	800	196.12 ± 03.37
4	6	26	1200	289.47±14.29
5	12	20	800	578.16±30.46
6	12	20	1200	595.12±13.78
7	12	26	800	554.12±37.91
8	12	26	1200	583.21±12.11

5.3.2. Optimization of formulation variables

Nanoparticles were prepared by using nanoprecipitation technique. Based on the solubility studies, phthalate buffers (pH 4.5) and F – 68 were selected as aqueous phase and stabilizer, respectively. However, the literature survey and the findings in our laboratory studies suggest that the formulation variables such as drug to polymer ratio and concentration of stabilizer could significantly alter the PS, PDI and EE of nanoformulations (Mainardes and Evangelista, 2005). Therefore, QbD based optimization of such formulation variables was taken up in this present research work with the help of expert design software. Nine batches were prepared as per 3^2 full factorial designs to optimize the two independent variables, drug to polymer ratio (A), stabilizer concentration (B) on responses such as PS (Y_1), PDI (Y_2) and EE (Y_3) of the BBR nanoparticles. The results are presented in Table 5.5. In this study, 1:2, 1:3 and 1:4 ratios were selected for optimization of the drug to polymer ratio. The amount of polymer was varied from 10 - 20 mg and amount of drug were kept constant at 5 mg in all the formulations to obtain the above ratios. These three different ratios were tested against stabilizer (F – 68) at 10, 25 and 50 mM.

Table 5.5. Results of EE, PS and PDI of formulations F1 – F9

Run	Formulations	Y_1	Y_2	Y_3
1	F-1	32.38 ±1.02	577.99 ±3.12	0.826 ± 0.01
2.	F-2	79.22 ±2.17	221.11±1.72	0.312 ± 0.02
3.	F-3	73.71 ±4.22	272.23 ±3.32	0.466 ± 0.034
4.	F-4	43.81 ±7.41	210.12 ±1.72	0.401 ± 0.021
5.	F-5	41.22 ±9.67	296.66 ±3.42	0.520 ± 0.022
6.	F-6	82.12 ±3.07	196.71 ±1.47	0.153 ± 0.012
7.	F-7	48.45 ±3.19	389.62±10.17	0.892 ± 0.034
8.	F-8	43.36 ±2.08	467.82±8.69	0.754 ± 0.026
9.	F-9	45.15 ±7.47	208.42±11.12	0.223 ± 0.018

5.3.2.1. Effect on entrapment efficiency

The entrapment efficiency (EE) of the nine formulations ranged from 32.38 ± 1.02 to 82.12 ± 2.07%. The constant and regression coefficients for EE (Y_1) as follows:

$Y1 = 79.38 -1.41 * A - 0.62 * B - 4.99 * A * B - 35.96 * A^2 - 1.57 * B^2$..... (1)

The quadratic model was found significant with F value of 23.16 (P = 0.0133). The value of r^2 coefficient was found to be 0.9747. In this case A^2 is the significant model term. The combined effect of the both of the factors elucidated with the help of contour and response surface plots (3D) shown in Figure 5.5 a. & b. The contour plots indicates that

optimized formulation (F – 6) is a blend of middle level of A (1:3) and higher level of B (50 mM) to get higher EE in nanoparticles. It was also demonstrated that adequate amount of polymer in dispersed phase plays a key role for higher entrapment efficiency. The poor EE of BBR observed in 1:2 of A is due to inadequate amount of polymer in organic phase. However, the poor EE in 1:4 ratio of A may be attributed to excess amount of polymer which may cause cohesiveness instead of adhesiveness.

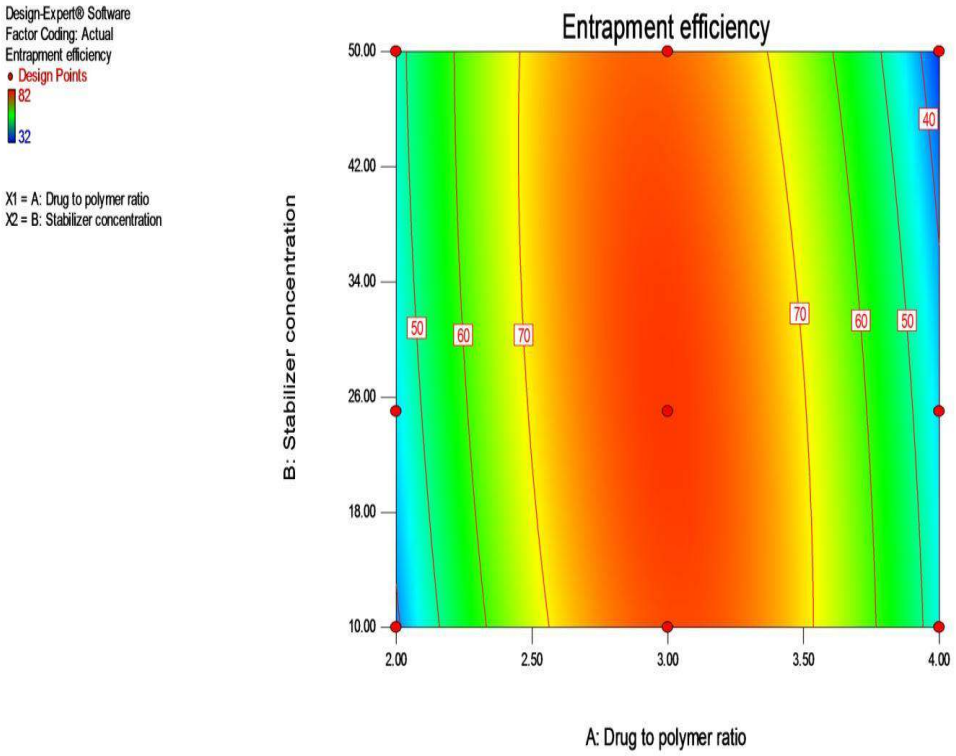

Figure 5.5.a. Contour plot of EE vs stabilizer concentration (mM) and drug to polymer ratio

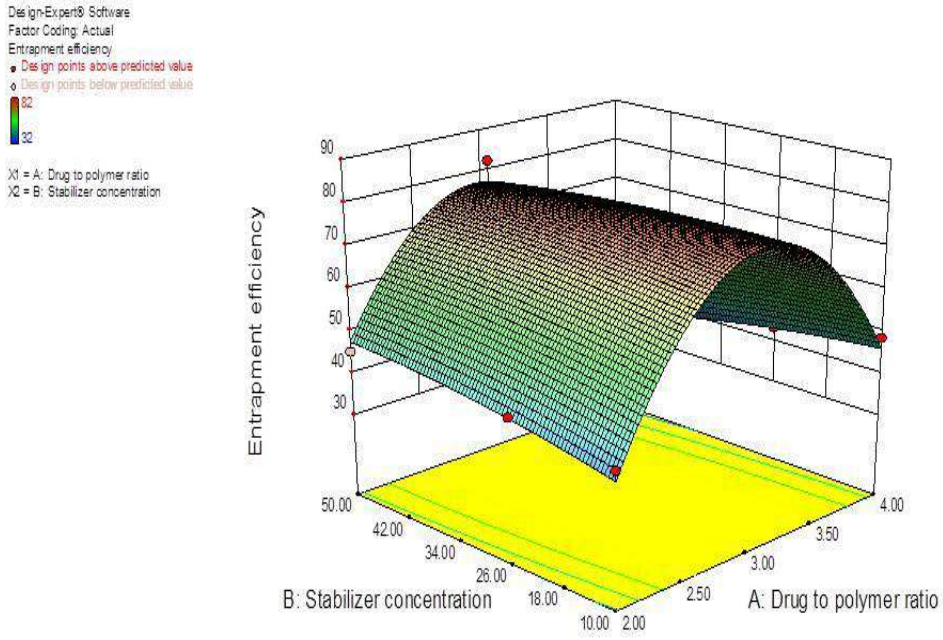

Figure.5.5.b. Response surface plot of EE vs stabilizer concentration (mM) and drug to polymer ratio

5.3.2.2. Effect on particle size and PDI

The particles sizes for nine batches obtained between 196 – 577 nm for nine batches. The constant and regression coefficients for PS (Y_2) were as follows:

$Y_2 = 213.57 + 125.60 * A + 4.11* B + 66.65 * A * B + 128.41 * A^2 + 24.41* B^2$..... (2)

The response surface quadratic model was found significant with F value of 12.65 (P = 0.0314). The value of r^2 coefficient was found to be 0.9547. In this case A and A^2 were significant model terms. The combined effect of the both of the factors elucidated with the help of contour and response surface plots (3D) are shown in Figure 5.6 a. & b. Contour plots

suggest influence of stabilizer concentration on particle size. Increasing of stabilizer concentration lead to decrease in the size of batches at drug to polymer ratios (1:2. and 1:3). It has been explained that higher concentration of stabilizer facilitated the formation of homogeneously dispersed smaller size of particles due to its surface tension reduction property. The formulation (F-6) showed lower particles size (196.71 nm). However, increase in the particle size was observed with batches (F-1, F-7 and F-8) containing drug to polymer ratio 1:4. It indicates that the concentration at 1:4 ratio of polymer results in the failure of the diffusion of organic phase into aqueous phase during precipitation process.

The polydispersity index of nine batches exhibited between 0.153 – 0.826. The constant and regression coefficients for PDI (Y_3) were as follows:

$Y_3 = 0.26 + 0.23^* A - 0.11 * B + 0.062 * A * B + 0.29 * A^2 + 0.056 * B^2$.....

(3)

The model was found significant with F value of 33.06 (P = 0.0080). The value of r^2 coefficient was found to be 0.9822. In this case A, B and A^2 were significant model terms. The combined effect of the both of the factors elucidated with the help of contour and response surface plots (3D) shown in Figure 5.7 a. & b. Contour plots indicates that formulation (F-6) showed narrow PDI (0.153). in this case the trend similar to particles size was observed.

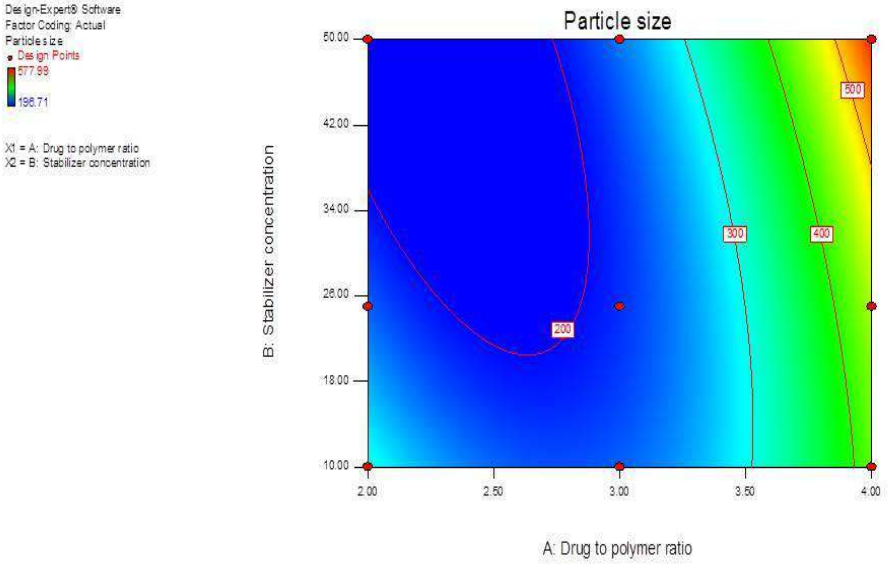

Figure 5.6.a. Contour plot of PS vs stabilizer concentration (mM) and drug to polymer ratio

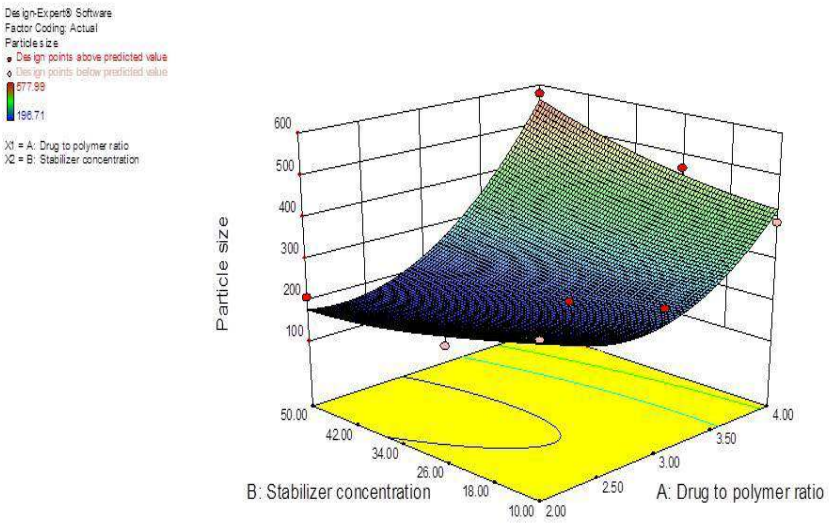

Figure 5.6.b. Response surface plot of PS vs stabilizer concentration (mM) and drug to polymer ratio

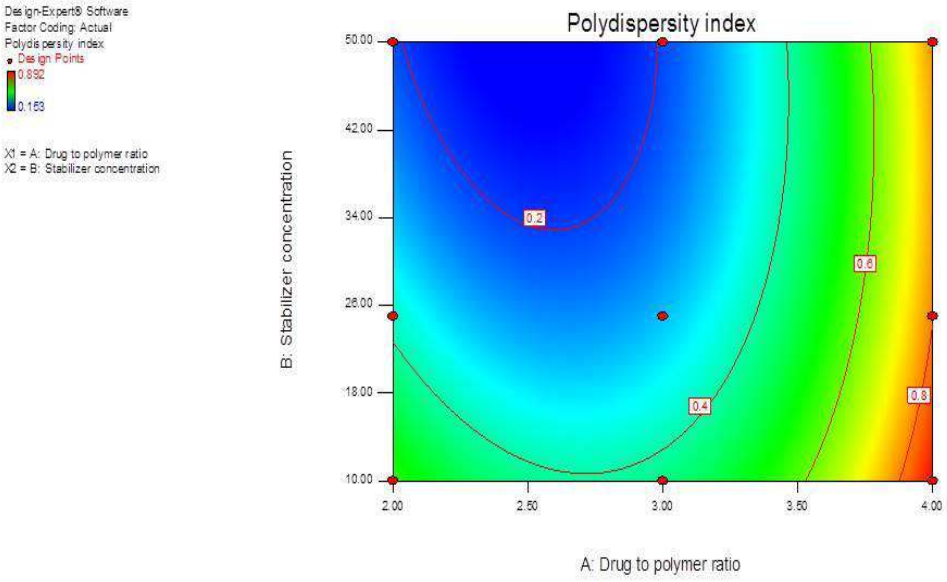

Figure 5.7.a. Contour plot of PDI vs stabilizer concentration (mM) and drug to polymer ratio

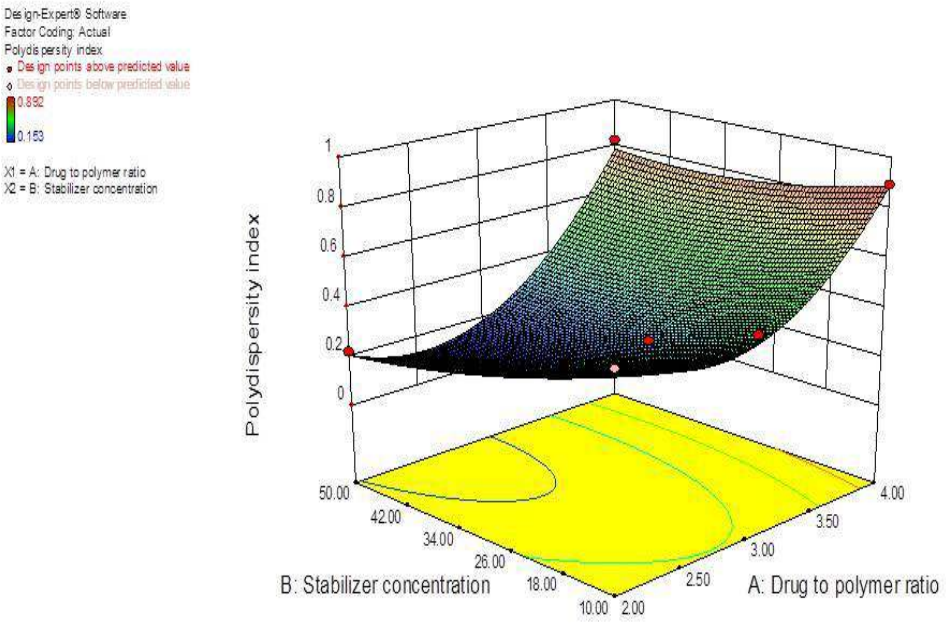

Figure.5.7.b. Response surface plot of PDI vs stabilizer concentration (mM) and drug to polymer ratio

The contour and response surface plots indicate that formulations with drug to polymer ratio (1:3) have higher entrapment efficiency. The results also explains that concentration of stabilizer at 50 mM not only facilitates the generation of homogeneous dispersed particles but also evade aggregation due to its enough surface tension reduction capacity (Koziara *et al.,* 2004). It also indicates that the formulation (F – 6), a blend of middle level of A (1:3) and higher level of B (50 mM) variable is optimized one with higher EE, lowest PS and narrow PDI. Moreover, the predicted and observed response variables of the formulation (F-6) with low percent of prediction error indicated the high prognostic ability of response surface model design for optimization. Thus, F-6 was selected as a final formulation (BBR-NP).

Nanoparticles were prepared by using nanoprecipitation method (Singh and Muthu, 2007). In brief, the polycaprolactone (PCL) was dissolved in acetone (organic phase) at 40°C and added to ethanolic solution of BBR. The organic phase was dropped into the stabilizer solution (aqueous phase) using glass syringe equipped with needle (gauge size 26) at the rate of 6 ml/min directly under magnetic stirring of 800 rpm at 25°C. The acetone was evaporated at 40 °C under reduced pressure, using a Rotary evaporator (IKA® RV 10 digital, Germany). The obtained nanodispersion was centrifuged at 15000 rpm for 30 min and obtained nanoparticles pellet was rinsed thrice with water. Finally, pellet was lyophilized using

lyophilizer (Lypholizer, Decibel, India) for 36 h at -40°C. The lyophilized nanoparticles were stored in desiccators until further use.

The surface coating was done by 1% w/v concentration of vitamin E TPGS. The slight increase in PS, PDI and changing of zeta potential of NP from negative to neutral region confirmed the successful surface coating. The data is shown in Table 5.6 and Figure 5.8 & 5.9 (a) and (b). The EE of the BBR in BBR-NP was found to be 82.12% and it was not significantly changed after its surface coating. It is expected that the addition of surfactants (stabilizers) can increase the solubility of drugs in aqueous medium due to its surface tension reducing property. During the surface coating, it may cause leaching of entrapped drug from NP during over night incubation period which may lead to reduction in entrapment of drug. Typically, it has been reported that surfactant property of vitamin E TPGS could not enhance the BBR solubility in aqueous medium (Battu *et al.*, 2010). Thus, it may be the probable reason for insignificant difference in EE of BBR NP after surface coating with vitamin E TPGS.

Table 5.6. Results of PS, PDI, ZP and EE of BBR-NP and BBR-SCNP

Type of NP	PS (nm)	PDI	ZP (mV)	EE (%)
BBR-NP	196.71 ± 4.47	0.153 ± 0.012	-26.3 ± 0.8	82.12 ± 2.84
BBR-SCNP	208.48 ± 1.07	0.166 ± 0.002	-10.32 ± 1.2	81.98 ± 1.29

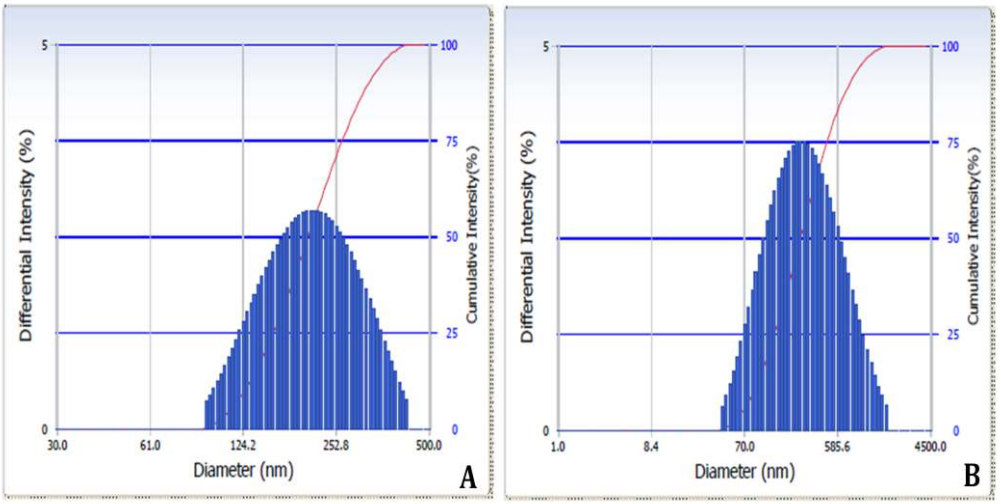

Figure 5.8. Particle size distribution of (a) BBR-NP and (b) BBR-SCNP

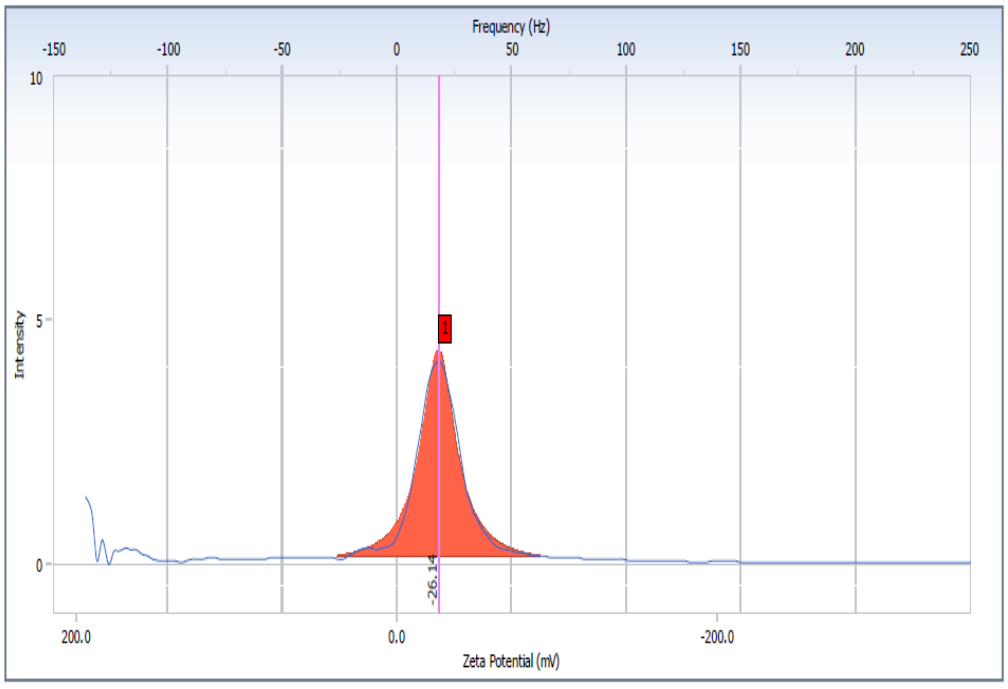

Figure 5.9. (a). Zeta potential of BBR-NP

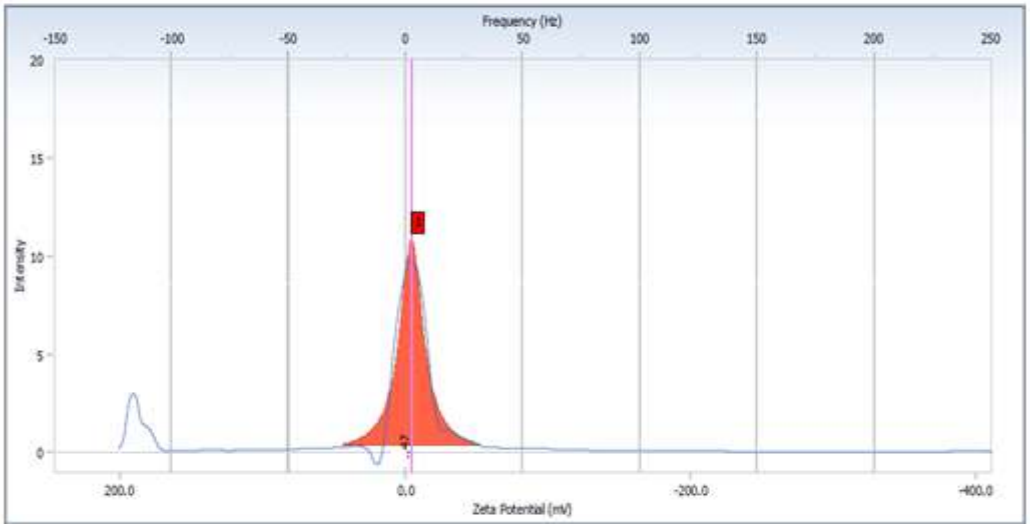

Figure 5.9. (b). Zeta potential of BBR-SCNP

5.4. Development of Naplet Technology

The naplets were prepared with naplet device. The naplets (3 mg BBR equivalent) was found to be almost of uniform weight 25 ± 2 mg and diameter 5 ± 0.2 mm. The sub coat and enteric coated naplets gained 27 ± 3 mg (approx. 6 %) weight. The prepared naplets without coating showed a slight rough surface texture whereas after coating the surface become smooth (Figure 5.10).

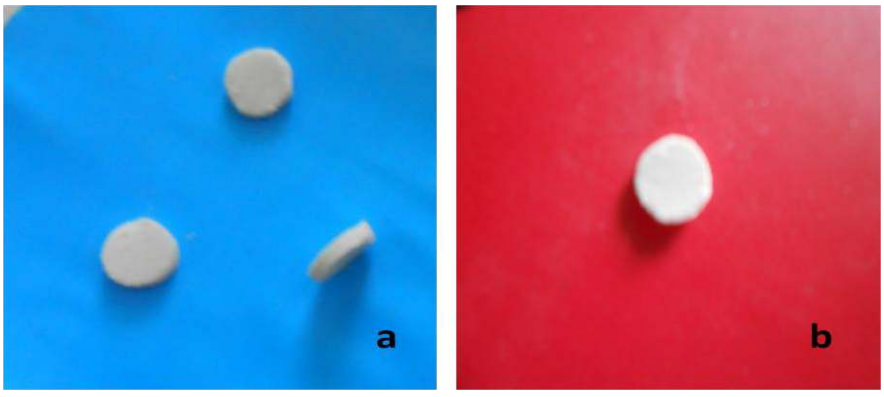

Figure 5.10. (a) uncoated naplet (b) enteric coated naplet

5.4.1. Optimization of binding and super disintegrating agents

Sodium starch glycolate and Povidone K-30 were selected as super disintegrating and binding agents, respectively. They have widely using in preparation of tablets. Binder is responsible for making of coherent mass where as disintegrating agent is responsible for breaking of naplet upon contact with dissolution medium. Therefore, the optimizations of binding and disintegrating agents are required in order to get rapid disintegration and good compact naplet. Thus, total 9 batches were prepared for optimization of concentrations of binding and disintegrating agents.

5.4.1.1. Effect on redispersion of nanoparticles

The results showed that 16 ± 5.9 to 90 ± 1.4 % of the nanoparticles were redispersed from respective batches of naplets as mentioned in Table 5.7. Redispersion was influenced by the amount of binder and disintegrating quantities. The observed poor redispersion in batches (3, 7, 8 and 9) is directly proportional to quantities of binding and disintegrating agents. The batch 5 exhibited higher redispersion compared to other batches. It indicates that quantities of binding and disintegrating agents at 0.50 mg w/w (2%) and 0.75 mg w/w (3%), respectively is optimum for better redispersion of nanoparticles.

The insignificant changes in PS, PDI and ZP of redispersed nanoparticles of naplet (batch 5) compared to initial BBR-NP dispersion was observed. The data is shown in Table 5.8. The SEM micro graphs of BBR-NP

dispersion indicate that nanoparticles are of spherical shape as shown in Figure 5.11. The shape remains spherical even after redispersion of the nanoparticles from naplet. The absence of aggregation of particles confirmed that nanoparticles were not undergoing any changes in shape either during mixing or in extrusion process of preparing naplet. Further, the particle size in micrographs also well correlated with the results of particle size analysis.

Table 5.7. Results of redispersion, hardness, friability and disintegration of different naplet batches

Batch	Redispersion (%)	Hardness (kg/cm^2)	Friability (%)	Disintegration (Sec)
1	68±2.4	3.1±0.46	1.212±0.71	52±3
2	52±3.7	6.8±0.57	0.078±0.03	69±2
3	37±2.2	11.2±0.33	0.047±0.46	108±5
4	87±1.1	2.8±0.69	1.429±0.17	26±2
5	90±1.4	5.2±0.93	0.059±0.02	29±2
6	46±1.7	10.45±0.38	0.033±0.16	131±4
7	29±3.6	3.5±0.52	1.486±0.52	152±6
8	21±2.3	6.6±0.23	0.047±0.11	148±4
9	16±5.9	13.5±0.84	0.042±0.18	164±6

Table 5.8. PS, PDI and ZP of BBR-NP dispersion and redispersed nanoparticles of naplet

Formulation	PS	PDI	ZP
BBR-NP dispersion	196.71±1.47	0.153± 0.004	24.11±1.47
Naplet	199.85 ±2.93	0.151 ±0.002	25.21 ±2.13

The TEM images of BBR-NP dispersion and redispersed nanoparticles (batch 5) also agreed with the results of SEM micro graphs and particle size analysis (Figure 5.12.). The TEM images showed that nanoparticle in dispersion or naplet are fairly spherical in shape and had no significant size difference between them.

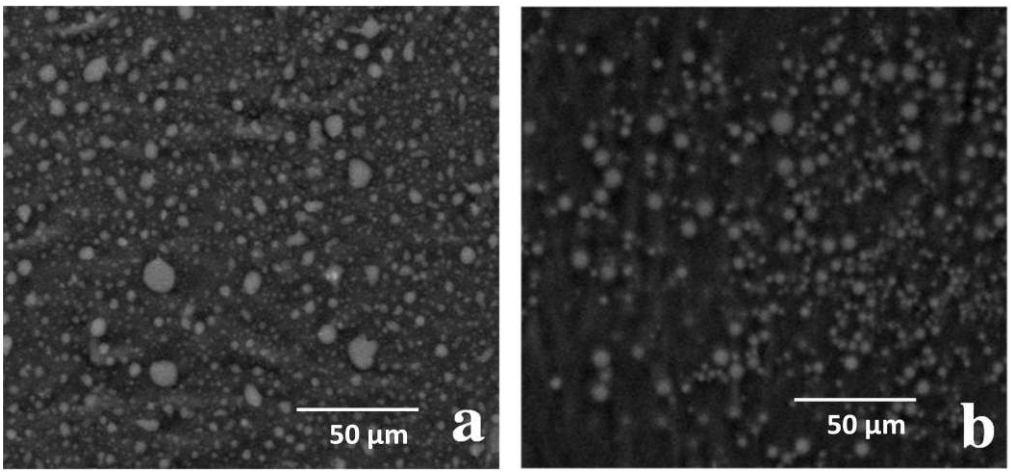

Figure 5.11. SEM micrographs of (a) BBR-NP dispersion (b) redispersed nanoparticles from naplet

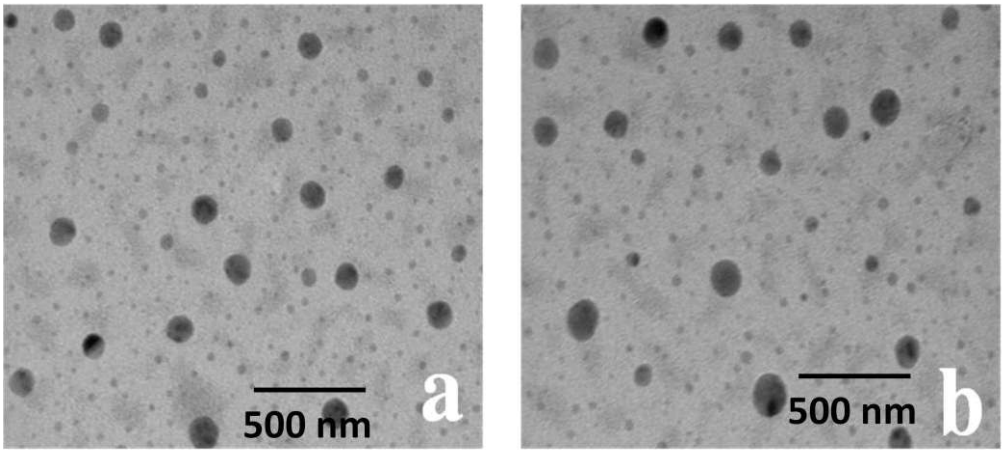

Figure 5.12. TEM images of (a) BBR-NP dispersion (b) redispersed nanoparticles from naplet

5.4.1.2. Effect on disintegration of naplet

The uncoated naplet of all batches were found to disintegrate in between 26 - 164 sec in water as mentioned in Table 5.7. The disintegration time depends on disintegrating and binder quantities. The batches (4 and 5) exhibited lesser disintegration time (26 and 29 sec) compared to other batches. It indicates that binder amount between 0.25 - 0.50 mg and disintegrating agent amount 0.75 mg are optimal quantities for fast disintegration of naplets. It was also observed that employing of higher quantities of disintegrating agent lead to delay in the disintegration of naplet and poor redispersion of nanoparticles. It may be due to formation of viscous gel layer at that quantity (1.25 mg) of SSG during contact with media (Bolhuis *et al.,* 1997).

The hardness of different uncoated naplet batches were shown between 2.8 ± 0.69 to 13.5 ± 0.84 Kg/cm^2. It was observed that increase in the

quantity of binder lead to increase in the hardness of naplet. The friability of uncoated naplet was between 0.033 ± 0.16 to 1.486 ± 0.52%. Similar to hardness, friability was also affected by the quantity of binder. The batches which were prepared with binder quantities (0.50 and 1.00 mg) exhibited permissible friability limits. It indicates that these batches could withstand the shear during coating, packing and shipping process. However, certain batches (1, 4 and 7) failed the friability test (more than 1% weight loss). It indicates that quantities of binder [0.25 mg (1%)] are inadequate to provide desired hardness to naplets.

The result of redispersion, disintegration, hardness and friability suggests that naplet (batch 5) is an optimized blend. Thus, uncoated naplet (batch 5) was selected as best naplet batch and subjected to sub and enteric coating. The hardness and friability of enteric coated naplets were 8.91±0.74 (kg/cm^2) and 0.018 ± 0.03 %, respectively**.** Increase in the hardness of the enteric coated naplet observed compared to uncoated naplet. The plasticity of enteric coated material might be reason for the increased hardness of coated naplet. Further, the enteric coated naplets does not disintegrate in pH 1.2 buffer up to three hours. This ensures that enteric coating (4%) is sufficient for preventing the release of either free adsorbed drug or nanoparticle from naplet in stomach region.

5.5. Characterization of nanoparticles (BBR-NP and BBR-SCNP)

5.5.1. FT-IR

The FT-IR spectra of pure BBR shows a methoxyl group peak appeared at 2844 cm^{-1} and the iminium (C=N+) double bond peak at 1635 cm^{-1} in the molecule [Figure 5.13 (a)]. Moreover, the peaks at 1569 cm^{-1} and 1506 cm^{-1} represent the aromatic C=C bending and the furyl group, respectively. The FT-IR spectra of physical mixture and berberine nanoparticles shows broad peaks without appearance of characteristic peak at 2844 cm^{-1} as depicted in Figure 5.13. (b) & (c). The other characteristic peaks of the drug also appeared in the range of 2000 cm^{-1} – 1500 cm^{-1} but with reduced intensities confirming successful entrapment of drug in PCL nanoparticles. Identical FT-IR spectra were obtained for placebo nanoparticles prepared in water and pH 4.5 buffers as shown in Figure 5.13. (d) & (e). These results revealed that the nanoparticles were stable and polymer might not be degraded in pH 4.5 buffers (selected aqueous phase) environment during the preparation.

The FT-IR spectrum of pure BBR revealed the existence of a methoxyl group peak appearing at 2836 cm^{-1} and the iminium (C=N+) double bond peak at 1606 cm^{-1} as shown in Figure 5.14. (a). Moreover, the peaks at 1569 cm^{-1} and 1506 cm^{-1} represent the aromatic C=C bending and furyl group, respectively. C-H peaks at 1719 cm^{-1} and 2857 cm^{-1} were identified in the IR spectra of PCL [Figure 5.14. (b)]. Characteristic

carbonyl functional group peak at 1657 cm^{-1} along with other characteristic C-O-C stretching vibrations of the repeated -OCH_2CH_2 chain of TPGS was observed in the region of 1104 – 1268 cm^{-1} as shown in Figure 5.14. (c) (Zheng *et al.*, 2013). Absence of characteristic peak of BBR at 2836 cm^{-1} confirmed successful entrapment of drug in nanoparticles as shown in Figure 5.14. (d). Further, presence of broad peaks with slight shifting at 1740 cm^{-1}, 2836 cm^{-1} of PCL and peaks at 1095 - 1227cm^{-1} of TPGS due to hydrogen bonding indicated coexistence of PCL and TPGS in surface coated NP. These results indicated that surface coating was done without chemical modification.

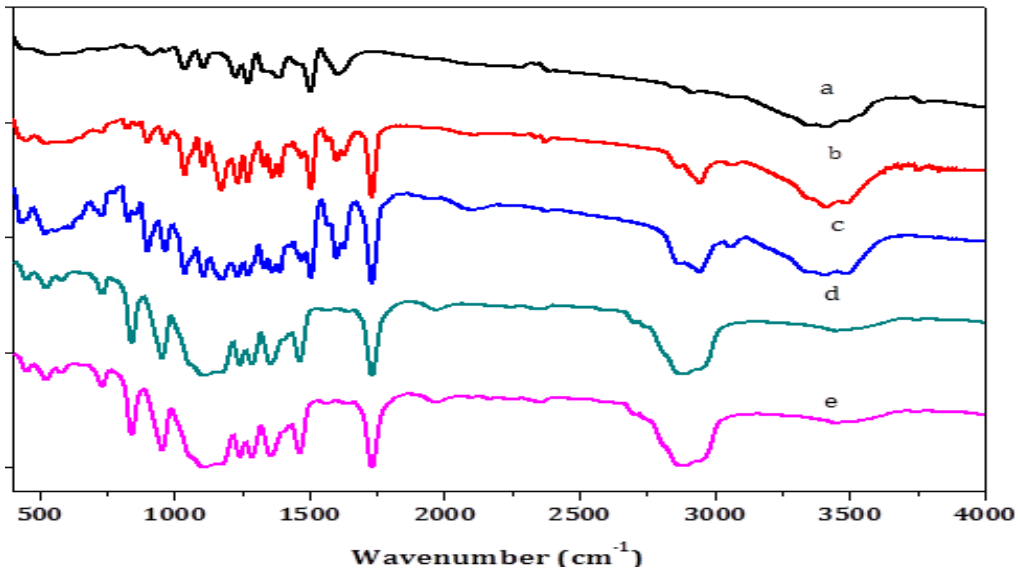

Figure 5.13. FT – IR spectra of (a) pure BBR (b) physical mixture of BBR and Polymer (c) BBR loaded NP (d) placebo NP prepared in water as a dispersion medium (e) placebo NP prepared in pH 4.5 phthalate buffer as a dispersion medium

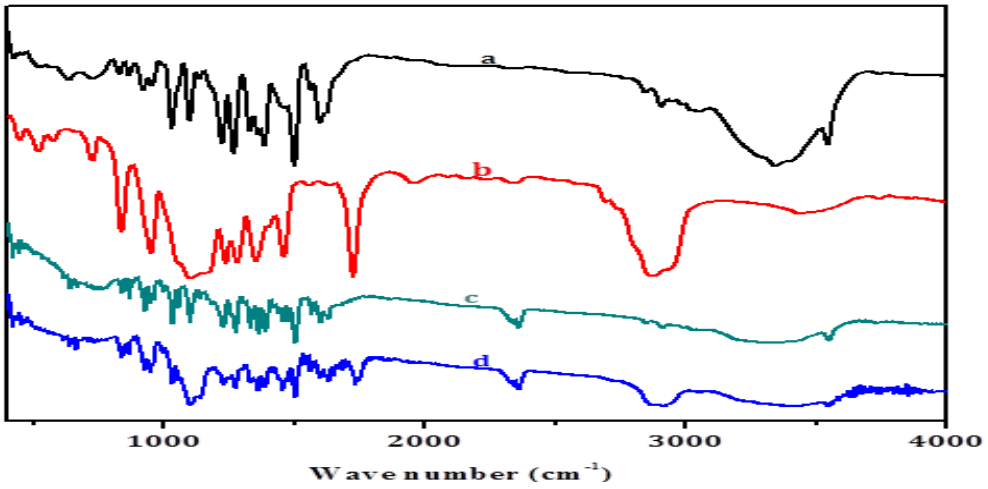

Figure 5.14. FT-IR spectra of (a) Pure BBR (b) PCL (c) TPGS (d) BBR-SCNP

5.5.2. DSC

DSC studies were performed in order to characterize state of drug in the nanoparticle formulation. The melting point of BBR is ~ 190°C and this appeared in the thermo gram of pure BBR along with other characteristic endothermic peaks which are depicted in Figure 5.15. (a) (Li and Xu, 2010). The characteristic sharp endothermic peak observed in thermo gram of the PCL at 55°C as shown in Figure 5.15. (b.). The disappearance of the characteristic endothermic peak of BBR and reduced intense peak of polymer at 55°C were observed in thermo grams of BBR loaded nanoparticles as shown in Figure 5.15. (c). The above results indicate that BBR was entrapped in nanoparticles and existed in amorphous state.

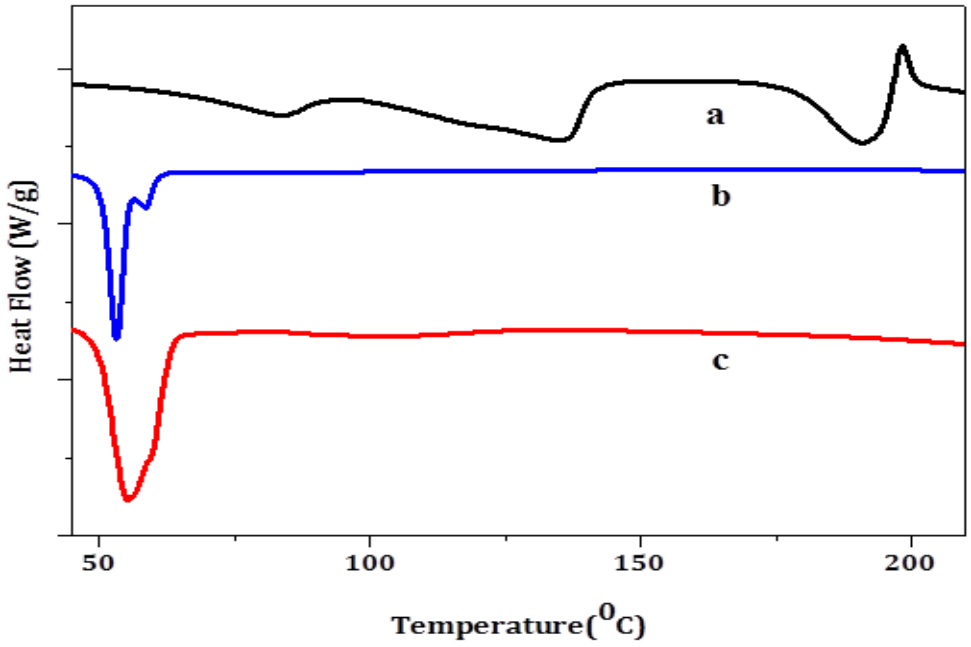

Figure 5.15. DSC thermo grams of (a) Pure BBR (b) PCL (d) BBR-NP

In addition, DSC studies were performed to confirm the surface coating of NP. It has been reported that the melting point of BBR, PCL and vitamin E TPGS are around ~ 190 °C, 55 °C and 40 °C, respectively (Mu and Feng, 2003; Moneghini *et al*., 2010; Li and Xu, 2010) . In this study, the melting point peak of BBR (~ 190°C) is appeared in the thermo gram of pure BBR along with other characteristic endothermic peaks [Figure 5.16. (a)]. The disappearance of the characteristic endothermic peak of BBR and appearance of PCL melting point peak at 55°C in thermo grams of BBR-NP confirmed that the BBR existed in amorphous state as shown in Figure 5.16. (b). In case of BBR-SCNP, the appearance of additional sharp endothermic peak of vitamin E TPGS at 32 °C without shift or arising of

new peaks indicates the coexistence of TPGS in BBR-SCNP as shown in Figure 5.16. (c). Thus, it can be concluded that vitamin E TPGS was present in BBR-SCNP without chemical modification with drug and PCL. The results of FT-IR also supported the DSC results of BBR-NP and BBR-SCNP.

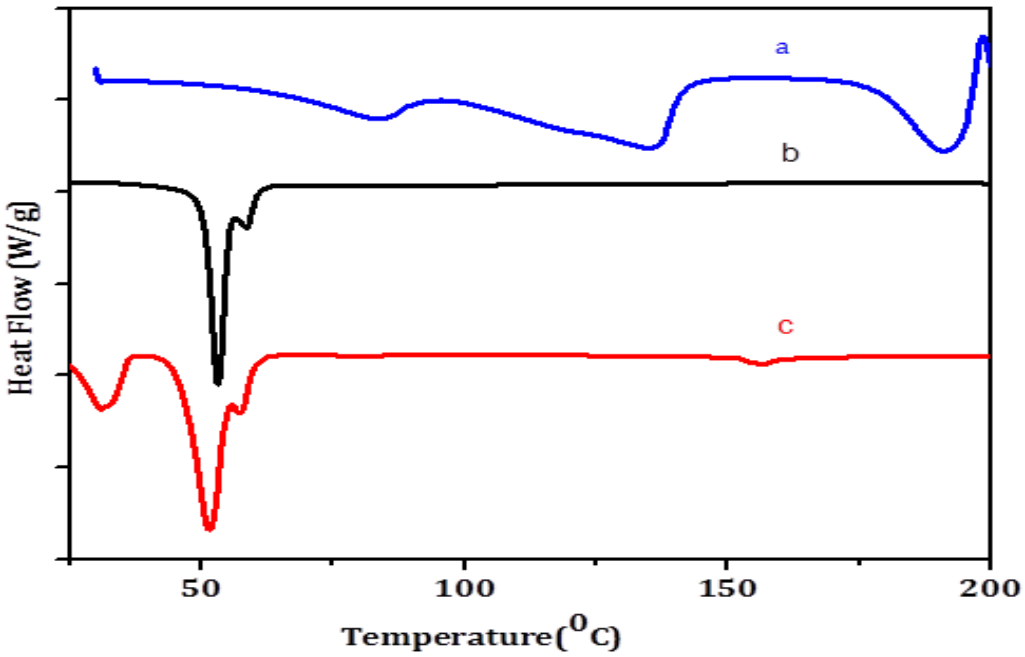

Figure 5.16. DSC thermograms (a) pure BBR (b) BBR-NP (c) BBR-SC NP

5.5.3. XRD

XRD patterns of BBR, PCL and lyophilized BBR-SCNP [Figures 5.17. (a), (b) & (c)]. XRD pattern of BBR exhibits sharp peaks which indicate crystalline nature of the drug. However, there are no characteristic peaks for lyophilized BBR-SCNP. This suggests that BBR was not in crystalline form and almost converted into amorphous form.

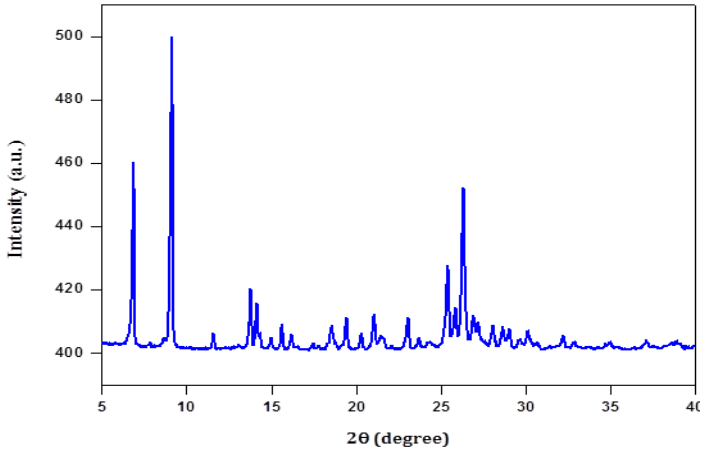

(a)

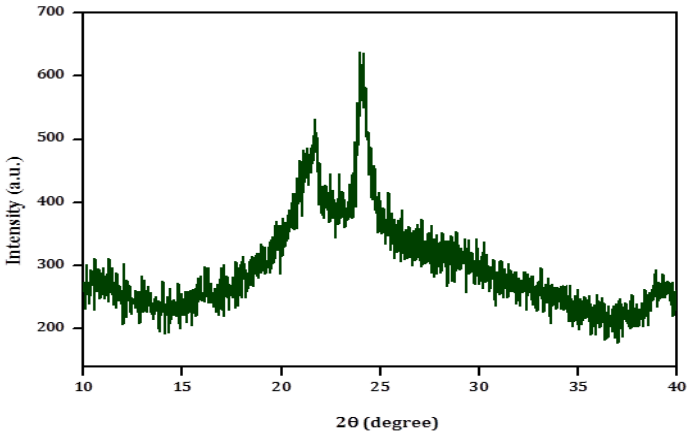

(b)

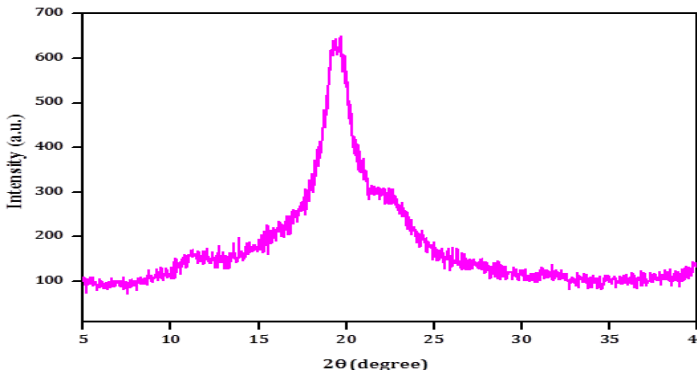

(c)

Figure 5.17. XRD patterns of (a) BBR (b) PCL (C) BBR-SCNP

5.5.4. TEM

Transmission electron microscopy was employed to verify the particle size results of both types of NP. TEM images are shown in Figure 5.18. (a) & (b). In TEM images, BBR-NP had spherical shape and smooth surface whereas BBR-SCNP exhibited steric layer on surface of the particle. The appearance of steric layer surrounding the surface of particle not only characteristically confirmed the surface coating but also differentiated surface morphology between BBR-NP and BBR-SC NP.

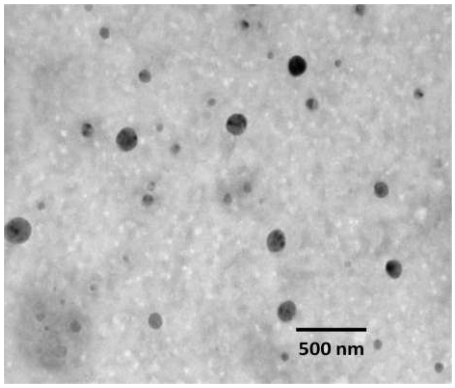

(a)

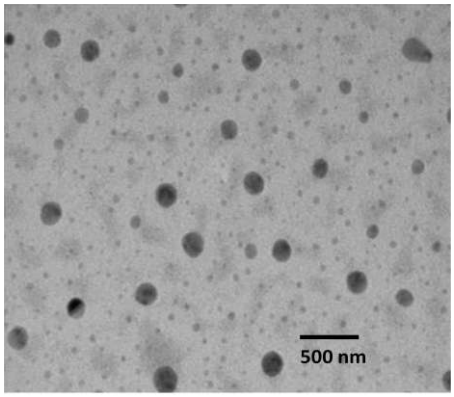

(b)

Figure 5.18. TEM images of (a) BBR-NP (b) BBR-SCNP

5.6. In-vitro drug release study

5.6.1. BBR NP and BBR-SCNP

In vitro release profiles of pure BBR and BBR-NP, lyophilized formulation (F - 6) in saline phosphate buffer (pH 7.4) are shown in Figure 5.19. Pure BBR showed rapid release, whereas formulation (F-6) exhibited biphasic release pattern with an initial burst release of adsorbed BBR on near the surface followed by sustained release of entrapped BBR from the NP. Pure BBR (3 mg) released more than 80% within 15 min. In case of formulation (F-6), nearly 82% of BBR was release in 24 h. The time required for 50% drug release (T_{50}%) of pure BBR solution and F-6 was found to be 0.14 h and 6.45 h, respectively. It may be due to the highly hydrophobic nature of PCL which retards the fast release of drug from the particle. Therefore, it is confirmed that optimized quantity of polymeric carrier is enough to facilitate the prolonged release of drug. The release data is fitted into Korsmeyer and Peppas equation and that the diffusion exponent (n value) was found to be 0.8391for formulation (F – 6). The n value is the diffusion exponent which characterizes the transport mechanism and the value less than 0.89 indicates anomalous diffusion or non-fickian diffusion (Peppas, 1985; Costa and Sousa Lobo, 2001). Anomalous diffusion or non-fickian diffusion refers to combination of both diffusion and erosion controlled rate release. Hence, the release mechanism of formulation (F – 6) was found to be non fickian diffusion.

In vitro release profiles of lyophilized BBR-NP and BBR-SCNP in saline phosphate buffer (pH 7.4) are shown in Figure 5.20. Both type of NP exhibited biphasic release pattern with an initial burst release of adsorbed BBR followed by sustained release of entrapped drug. Both types NP, nearly 82% of BBR released in 24 h. The time required for half quantity of drug release (T_{50}%) for both type of NP were found to be 6.34 h and 6.45 h, respectively. Highly hydrophobic nature of PCL may retard the fast release of drug from the NP. The release data is fitted into Korsmeyer and Peppas equation and the diffusion exponent (n value) was found to be 0.8791 for BBR-SCNP. The n value is the diffusion exponent which characterizes the transport mechanism and the value less than 0.89 indicates anomalous diffusion or non-fickian diffusion. Hence, the release mechanism of BBR-SCNP was found to be non fickian diffusion.

5.6.2. Naplet

Comparative *In-vitro* release profiles of BBR-NP dispersion and naplet in pH 1.2 and pH 6.8 are shown in Figure 5.21. It was observed that in pH 1.2, the drug 41% was released from BBR-NP where as no release of drug was observed from enteric coated naplet up to 3 h. BBR-NP dispersion and naplet exhibited sustained drug release pattern in pH 6.8 dissolution medium. The 82 % and 75% of the drug was release from BBR-NP dispersion and naplet in 24 h, respectively. The time required for 50% drug release (T_{50}%) from BBR-NP dispersion and naplet were found to be

8.04 h and 11 h, respectively. However, delay in initial burst release was observed at pH 6.8 in naplet compared to BBR-NP dispersion. It may be due to the lag period for disintegration of naplet.

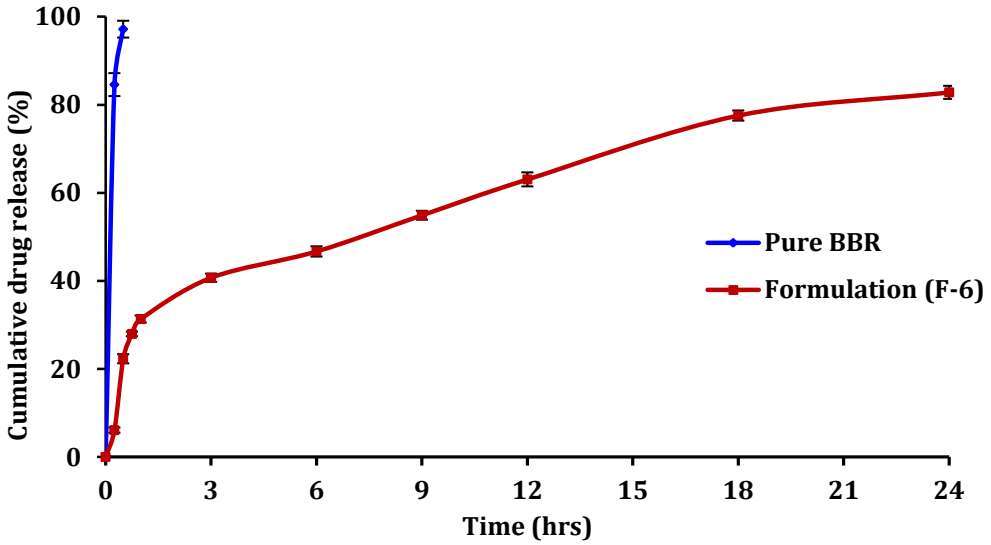

Figure 5.19. *In – vitro* release study of pure BBR solution and formulation (F – 6) in PBS medium (pH 7.4)

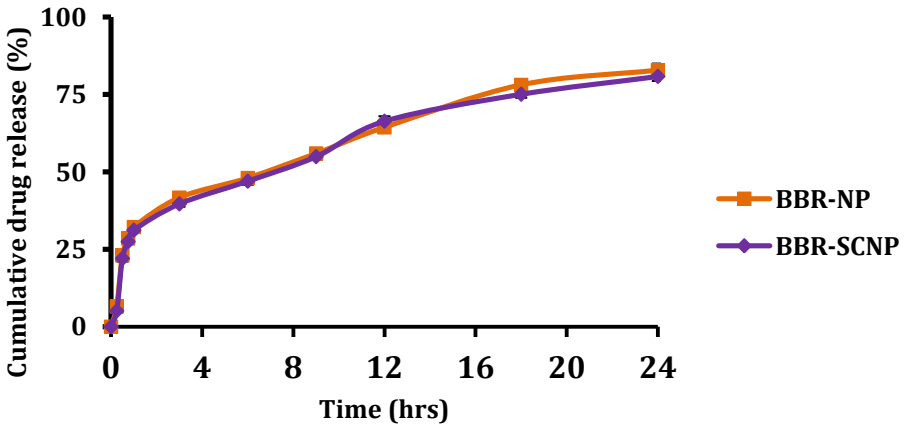

Figure 5.20. *In-vitro* drug release profile of BBR-NP and BBR-SCNP in PBS medium (pH 7.4)

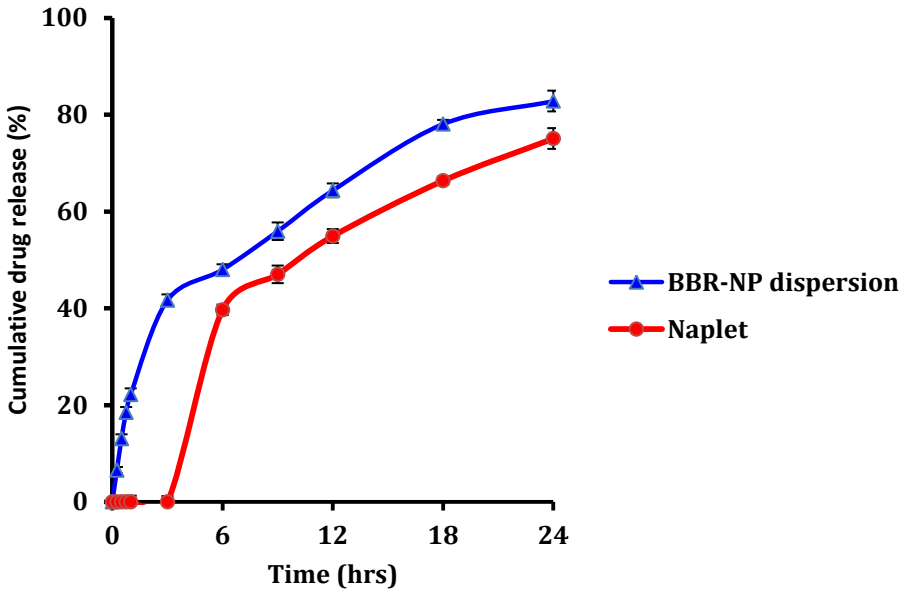

Figure 5.21. *In-vitro* drug release profile of BBR-NP dispersion and naplet in pH 1.2 (hydrochloric acid buffer) and pH 6.8 (phosphate) medium

5.7. Stability studies

5.7.1. Study at storage conditions (shelf life)

Stability studies of finally selected BBR-NP lyophilized formulation (F – 6) was carried out over a period of 180 days at 25 ± 2°C/60 ± 5 % RH storage condition. Lyophilized formulation was reconstituted with water into nanodispersion and then characterized for PS, PDI, ZP, EE and drug release. There was no significant (P> 0.05) difference observed throughout the stability period in above parameters. Data is shown in Table 5.9. It is indicates that optimized stabilizer concentration (50 mM) was sufficient for stabilization of nanoparticles. Formulation (F-6)

showed insignificant change in drug release either during burst release phase or sustained release phase (Figure 5.22). Thus, the above results indicate that lyophilized nanoparticles were stable at 25 °C storage condition.

Stability studies of lyophilized BBR-SCNP was carried out to evaluate the changes in parameters such as PS, PDI, zeta potential, EE and drug release over a period of 180 days at cool temperature (8°C). There was no significant (P> 0.05) difference observed throughout the stability period in above parameters. Data is shown in Table 5.10.

Table 5.9. Stability studies of BBR-NP formulation (F-6)

Parameters	(0) Days	(180) Days
Particles Size	196.71±1.47	198.46±1.62
Polydispersity Index	0.153 ± 0.002	0.151 ± 0.004
Zetapotential (mV)	-24.11±1.47	-22.56±1.96
% Entrapment Efficiency	82.12±3.07	81.42±4.31

Table 5.10. Stability studies of BBR-SCNP formulation

Parameters	(0) Days	(180) Days
Particle Size (nm)	208.48 ± 1.07	209.23 ± 1.21
Polydispersity index	0.166 ± 0.04	0.164 ± 0.02
Zetapotential (m.V)	-10.32 ± 1.2	-10.37 ± 0.92
Entrapment efficiency (%)	82.12 ± 3.07	81.42 ± 4.31

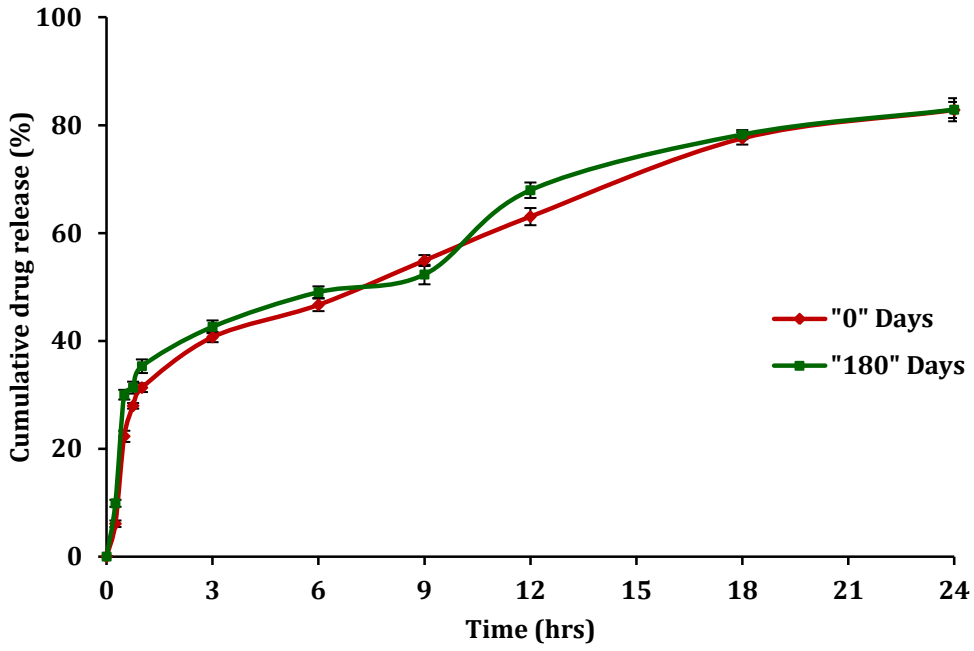

Figure 5.22. Comparative *In – vitro* release study of nanoformulation (F-6) in PBS medium (pH 7.4) at "0" and "180" days

Stability studies of naplet was carried out over a period of 180 days at 25 ± 2°C/60 ± 5 % RH storage condition and evaluated the changes in parameters such as PS, PDI, zeta potential, hardness, friability and disintegration time. There was no significant (P> 0.05) difference observed in above parameters throughout the stability period. Data is shown in Table 5.11. Thus, the above results indicate that naplet is stable at 25 °C storage condition.

Table 5.11. Stability studies of naplet

Parameter	0 day	180 day
Redispersion (%)	90 ± 4	88 ± 3
Redispersed nanoparticle size (nm)	196.71 ± 1.47	198.46 ± 1.62
Polydispersity index	0.153 ± 0.012	0.161 ± 0.017
Zetapotential (mV)	-24.11 ± 1.47	-22.56 ± 1.96
Hardness (kg/cm²)	8.91 ± 0.74	8.11 ± 1.86
Friability (%)	0.148 ± 0.03	0.139 ± 0.092
Disintegration (sec)	26 ± 3	29 1

5.7.2. Stability study in simulated biological fluids

The pre and post incubated BBR-NP and BBR-SCNP in SBF pH 6.8 and 7.4 with or without sodium taurcholate (20 mM) and human plasma were characterized for their PS, PDI and ZP. Data is shown in Table 5.12. The PS, PDI and ZP of BBR-NP and BBR-SCNP (without incubation) were 190.71 ± 4.47 nm and 208.48 ± 1.07 nm; 0.116 and 0.166; -26.3 ± 0.8 mV and -10.32 ± 1.2 mV), respectively. After incubation of BBR-NP in SBF pH 6.8 and 7.4 for 30 min there was observed the particle size (2234.60 ± 458.63 nm and 3189.43 ± 87.12 nm), respectively PDI (0.509 and 0.721), respectively and zeta potential (-02.35 ± 0.9 mV and -01.92 ± 0.7 mV), respectively. The increase in PS and PDI of BBR-NP in pH 6.8 and 7.4 (mimics the micro environments of intestinal region and systemic circulations) may be due to agglomeration. Usually, the zeta potential of

uncoated NP (-26. mV) would be enough to prevent aggregation and maintain their stability at storage conditions. However, the changes in ZP of BBR-NP from negative to neutral charge during incubation may have resulted in failure of its Brownian motion leading to aggregation and increase in particle size. This also reflects that the potential charge of particles in corresponding pH environment at which surface charge inspired electrostatic repulsion forces could not overcome the Vander Waals attractive forces and eventually developed the tendency to agglomerate. Interestingly, insignificant changes in PS, PDI and zeta potential observed with BBR-NP when incubated in SBF (pH 6.8) with STC of 20 mM. It may be due to the facilitation of appropriate alkaline environment by STC which prevents the agglomeration of negatively surface charged NP. It has been reported that in alkaline environment negatively charged NP are more stable than positively charged NP (Lu *et al*., 2007; Iijima and Kamiya, 2009). On other hand, significant difference in PS, PDI and insignificant changes in ZP were observed with BBR-NP after incubation in human plasma. It may be due to the adsorption of protein corona on surface of NP. A group of plasma proteins are called as protein corona (Yallapu *et al*, 2011). Further, the insignificant change in zeta potential indicated that the adsorbed protein corona were bonded to the surface of NP due to hydrophobic nature and charge interactions but were not involved in agglomeration of NP and subsequent instability.

Therefore, increase in PS is not due to agglomeration of NP but due to adsorption of protein corona.

The vitamin E TPGS surface coated NP showed insignificant differences in PS, PDI and ZP and exhibited good stability (no agglomeration) at post incubation in similar conditions for the same time (30 min) due to its steric stabilization or stealth property. In surface coating, a tiny steric layer could be formed on surface of core particle which prevents the tendency of agglomeration due to electrostatic repulsion even at neutral zeta potential region.

Transmission electron microscopy was employed to verify the particle size results of both types of NP which were observed at pre and post incubation conditions. TEM images are shown in Figure [5.23. (a), (b), (c) & (d)]. In TEM images, BBR-NP had spherical shape and smooth surface whereas BBR-SCNP showed steric layer on surface of the particle. The appearance of steric layer surrounding the surface of particle not only characteristically confirmed the surface coating but also differentiated surface morphology between uncoated and surface coated NP. Particle aggregates were observed in TEM image of BBR-NP when they were incubated with SBF (pH 6.8) and this corroborated well with the results of particle size [Figure 5.23.(a)]. Slight rough surface and heterogeneous particles without aggregation were observed in TEM images of BBR-NP which were incubated in plasma. It may be due to addition of protein

corona on surface of the uncoated NP. However, TEM images correlated well with particles size results and showed addition of the protein corona. It might be appropriate reason for significant increase in particle size of BBR-NP [Figure 5.23.(b)]. However, the agglomeration and heterogeneous particle sizes were not observed in TEM images of BBR-SCNP at specified incubation conditions. The TEM images evidently demonstrated that the non-ionic steric stabilization and surface hydrophilicity of vitamin E TPGS plays a role in prevention of agglomeration and maintains stability at specified incubated conditions. The results of particle size and TEM images revealed that surface coating by vitamin E TPGS (1% w/v) prevented the agglomeration of BBR NP when exposed to different SBF conditions.

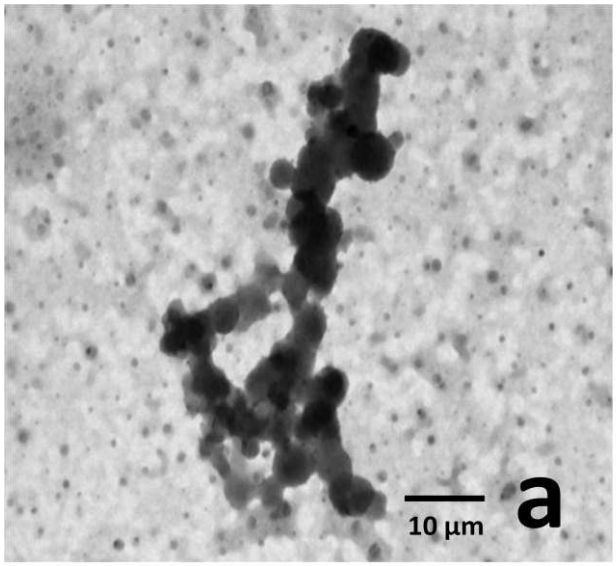

(a)

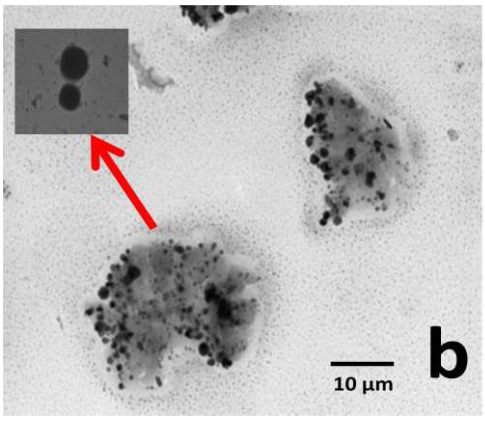

(b)

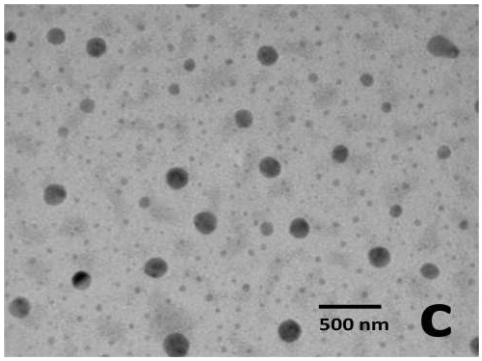

(c)

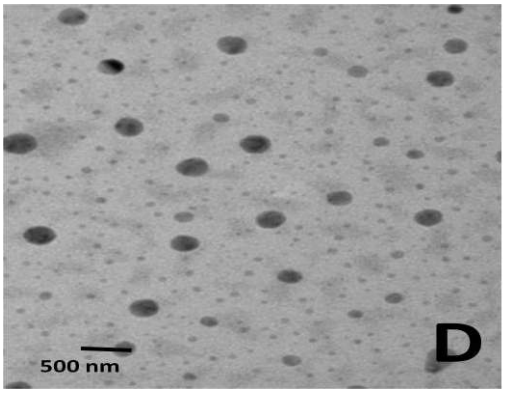

(d)

Figure 5.23. TEM images (a) BBR-NP in SBFs (pH 6.8) (b) BBR-NP in plasma (c) BBR-SC NP in SBFs (pH 6.8) (d) BBR-SCNP in plasma

Table 5.12. Results of BBR-NP and BBR-SCNP after 30 min of incubation in SBFs at different pHs

Incubation Medium	Type of Nanoparticle	Particle Size (nm)	Zeta potential (mV)
Without incubation	BBR-NP	190.71 ± 4.47	-26.3 ± 0.8
	BBR-SCNP	208.48 ± 1.07	-10.32 ± 1.2
SBF pH 6.8	BBR-NP	2234.60 ± 458.63	-02.35 ± 0.9
	BBR-SCNP	206.23 ± 08.11	-09.32 ± 1.2
SBF pH 7.4	BBR-NP	3189.43 ± 87.12	-01.92 ± 0.7
	BBR-SCNP	212.84 ± 09.31	-09.17 ± 0.8
SBF pH 6.8 with Bile Salts STC (20 mM)	BBR-NP	201.47 ± 21.10	-23.81 ± 1.4
	BBR-SCNP	213.56 ± 02.36	-10.64 ± 3.1
Plasma	BBR-NP	586.12 ± 51.23	-24.61 ± 2.2
	BBR-SCNP	207.43 ± 06.17	-08.19 ± 0.7

5.8. Pharmacokinetic study

5.8.1. HPLC bio-analytical method development

Plasma calibration curve of BBR was linear over the range 100 - 1000 ng/ml and the retention of BBR was 7 min. The regression equation was y = 34.71 x – 115.43 and mean correlation coefficient (R^2) was 0.9999. The accuracy (% of recovery) values of 50, 500 and 1000 ng/ml from blood plasma were 80.3%, 87.6% and 88.4%, respectively. The coefficients of variation (CV) for intra and inter day precision were less than 10%, and the LOQ was 55.23 ng/ml, and LOD was 15.91 ng/ml. The validation parameters are presented in Table 5.13. A representative chromatogram of BBR and calibration curve obtained from the HPLC analysis is shown in Figure 5.24 and 5.25.

Table 5.13. HPLC bio analytical method validation parameters

Parameters		Results
Range		100 -1000 ng/ml
Regression equation		y = 3.471x - 115.43
Regression coefficient (R^2)		0.999
Accuracy (% Recovery)		97.57±1.16
Precision (% CV)	Intra-Day	1.31±0.97
	Inter-Day	1.74±0.61
LOD (ng/ml)		15.91
LOQ(ng/ml)		55.23

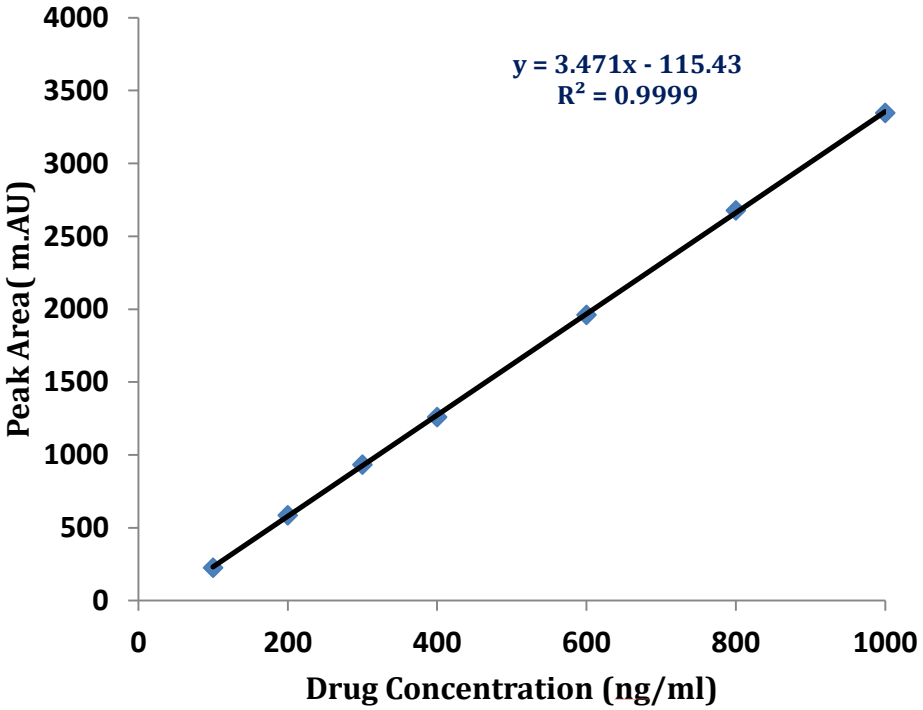

Figure 5.24. Standard curve of berberine in plasma

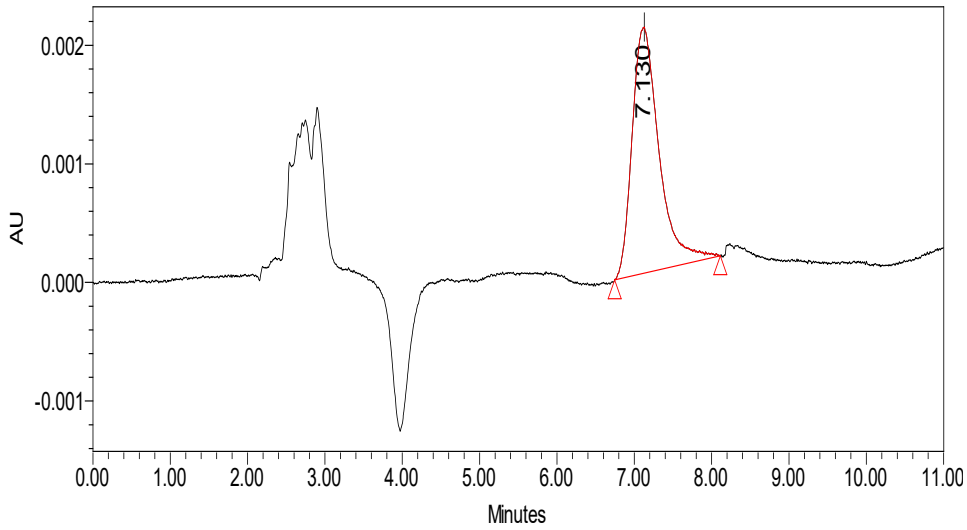

Figure 5.25. Chromatogram of Berberine in plasma

5.8.2. Oral single dose animal study

Plasma concentration – time curves of single dose pharmacokinetic study results are shown in Figure 5.26. Different pharmacokinetic parameters are tabulated in Table 5.14. The C_{max} of BBR-NP (5.977 ± 0.166 µg/ml) was significantly different compared to BBR aqueous solution but insignificantly with BBR-SCNP. The AUC of BBR-NP was 3.23 and 1.52 folds higher compared to BBR aqueous solution and BBR with verapamil group, respectively. It indicates that encapsulation of BBR in nanosize form enough to circumvention of P-gp efflux effect. BBR-NP showed pharmacokinetic parameters (C_{max} and AUC) which are near to BBR-SCNP. However, the difference in values of $T_{1/2}$ and clearance indicate that surface coating with vitamin E TPGS not only avoids the P-gp efflux at its absorption site (intestine) but also at organs which are responsible for metabolism and excretion (kidney and liver). Moreover, surface coating with hydrophilic agent avoids the binding of proteins and subsequent opsonization lead to longer retention of nanopartices. It may also be the reason for decrease in clearance of BBR-SCNP. The AUC of BBR-SCNP was significantly higher compared to all other groups. The bioavailability of BBR was enhanced 3.5 folds in BBR-SCNP compared to BBR aqueous solution and it was also 1.7 folds higher than group which was treated with BBR and verapamil (P-gp inhibitor). The results indicate that administration of BBR in surface coated nanoformulation would be

beneficial for enhancement of its bioavailability and longer retention in systemic circulation.

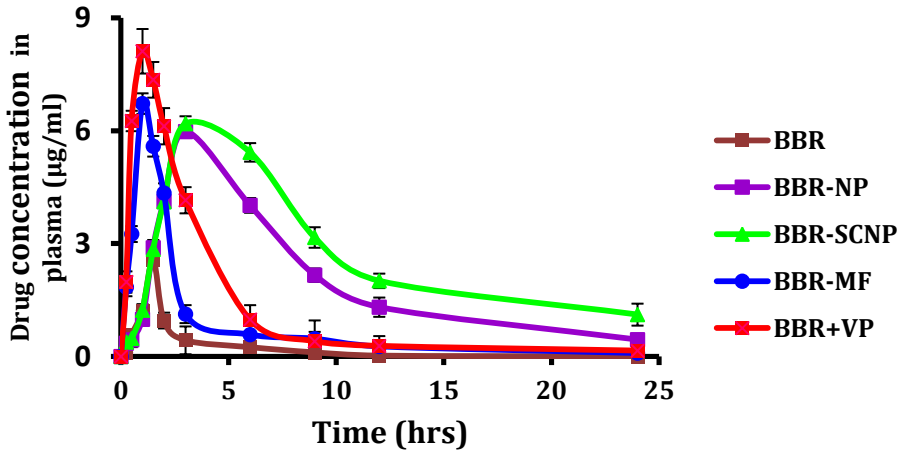

Figure 5.26. Results of Plasma concentration – time curves of single dose pharmacokinetic study

Table 5.14. Pharmacokinetic parameters of different animal groups

Pharmacokinetic parameters	BBR	BBR-NP	BBR-SCNP	BBR-MF	BBR + VP
C_{max} (µg/ml)	2.569 ± 0.140	5.977 ± 0.166 a	6.187 ± 0.197 b/e	6.722 ± 0.213	8.112 ± 0.513
T_{max} (µg/ml)	1.57± 0.10	3.10± 0.07	3.27± 0.12	1.20± 0.11	1.10± 0.11
$T_{1/2}$ (hr)	2.037± 0.12	6.893± 0.15	10.863± 0.09	6.63± 0.11	11.68± 0.10
AUC (hr x µg/ml)	14.947± 1.25	48.305± 1.03	52.317± 0.98 a/b/c/d/e	17.82± 1.22	30.67± 1.27 c
Cl (mL/min/kg)	341.72± 12	31.589± 5	20.134± 8.1 a/b/c/d/e	83.61± 9.21	50.04± 10.27

a= BBR vs BBR-NP, b=BBR vsBBR-SCNP, c=BBR vsBBR-MF, d=BBR vs BBR+VP, e=BBR-NP vs BBR-SCNP

5.9. Haemocompatibility study

5.9.1. Haemolysis assay

Haemolysis is one of the rapid red blood cell burst processes. It may spontaneously occur at intolerable micro environment condition. It is one of the significant parameter reflecting the incongruity with foreign material as well as with acute toxicity. Occurrence of haemolysis mainly depends on the following impact such as net surface charge of the particle and chemical composition of the used material/excipeint. It may also greatly affect the surface to volume ratio (macro – micro – nano) as compared to their respective bulk materials (Koziara *et al*., 2005 and Mayer *et al*., 2009). Thus, it becomes obligatory to evaluate the haemocompatibility of developed novel formulations. Particularly, it needs more attention in case of development of nanoparticulate delivery systems for drugs as nanoscale size of particle can interact easily with micron sized red blood cell and may initiate rapid haemolysis if materials are incompatible.

The results of haemolysis assay are shown in Figure 5.27. Haemolysis test indicates that all samples had permissible haemolysis where as pure BBR (100 µg/ml) showed higher haemolysis but within the limits (<10%) when compared against positive control (assumed100%) (Amin and Dannenfelser, 2006). The surface charge based interaction between positively charged drug and negatively charged red blood cells may be

the appropriate reason for observed higher haemolysis in case of pure BBR at 100 µg/ml. Both type of BBR loaded NP equivalent to 100 µg/ml did not show haemolysis because entrapped drug had facilitated lower exposure of drug to RBC even at similar bulk volume ratio of pure BBR. Previous reports indicate that interaction of cationic charged particles or drug with anionic charge RBC causes haemolysis. Electro repulsion between negative charge of the naked NP or neutral charge of the TPGS surface coated NPs with negatively charged blood cells may be a probable reason in avoiding the interaction between them and thus the subsequent haemolysis. As a result, surface coating with non ionic (neutral charge) natural excipients like TPGS may be beneficial in prevention of haemolysis and improves the NP blood compatibility due to its non-interference in charge based interactions. The results of drug, uncoated, surface coated BBR and placebo NP showed that net charge and exposure of the bulk volume of the NP into RBC medium are found to be critical factors in haemolysis. The present study reveals that composition and concentration of both type of NP with and without drug are found to be suitable for systemic administration.

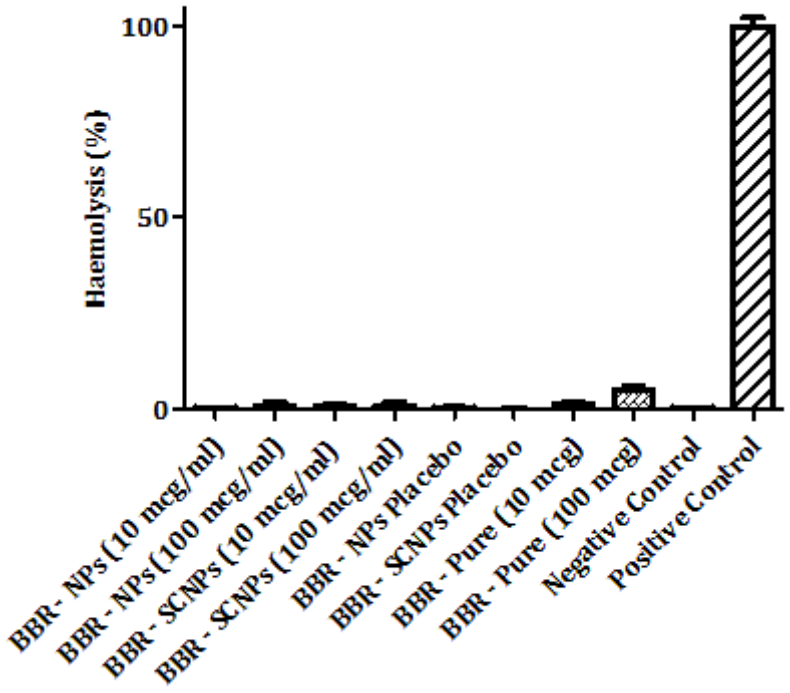

Figure 5.27. Haemolysis results of BBR-NP, BBR-SCNP and placebos after incubation in blood

5.9.2. LDH assay

Erythrocyte membrane integrity was evaluated by LDH assay. This assay was intended particularly for evaluation of the influence of vitamin E TPGS on erythrocyte membrane integrity. The assay results are shown in Figure 5.28. All the samples exhibited insignificant increase in release of LDH enzyme compared to negative control. However, BBR (100 µg/ml) sample released higher level of LDH enzyme when compared to other samples. It may be due to the bulk exposure of the pure BBR (100 µg/ml) at specified RBC suspension volume and net charge interaction between

them. This indicates that presence of higher quantities of BBR in blood may lead to adverse effects. On other hand, significant difference in LDH release between pure BBR and drug loaded NP at 100 µg/ml quantities revealed that encapsulation of drug in NP and its surface coating not only improved the stability in relevant media but also reduced adverse effects associated with bulk exposure of drug in blood. Further, these observations are also in conformity with the haemolysis results.

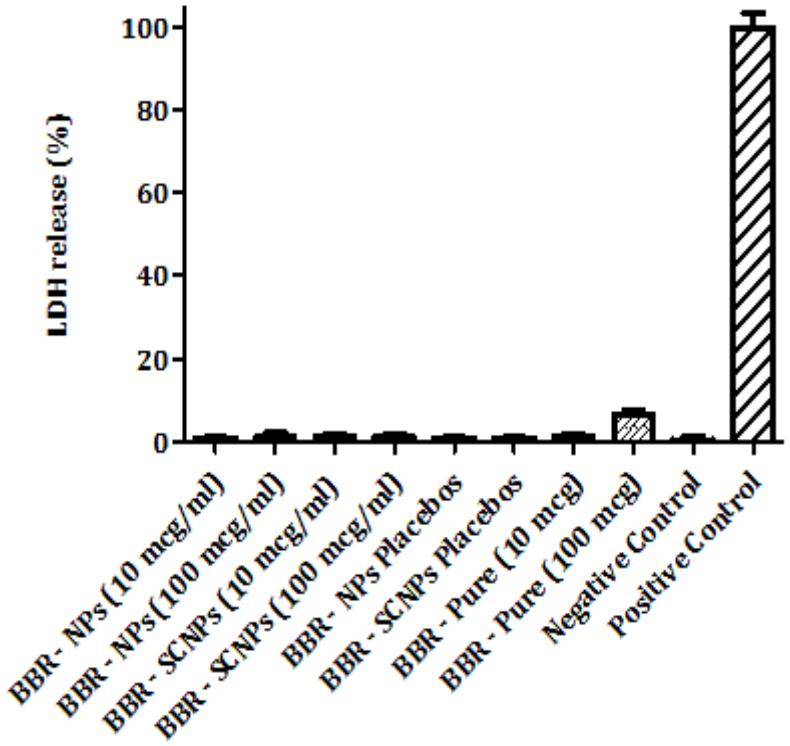

Figure 5.28. LDH assay results of BBR-NP, BBR-SCNP and placebos after incubation in blood

5.9.3. Platelet aggregation

The interaction of platelets in blood samples with different NP and pure BBR samples were qualitatively studied by light microscopy after incubation of samples. Primarily, blood smears were prepared for the samples and stained as per procedure. The stained samples were observed microscopically for qualitative visual confirmation. The microscopic images are shown in Figure 5.29. The platelets observed in microscopic images were indicated in round circles. There was no platelet aggregation in microscopic images of all samples. In certain conditions, exposure of higher quantity of drug may cause platelet aggregation. In this study even pure BBR (100 µg) did not shown such kind of platelet aggregation. It may be due to the anti-platelet aggregation property of BBR. Thus, the results confirmed that there was no impact of drug, polymer and vitamin E TPGS at used quantities for platelet aggregation. In addition, the blood samples were quantitatively evaluated for platelet count by auto hematological counter. All samples were in normal range as shown in Figure 5.30.

Thus, the quantitative and qualitative results of above haemocompatibility studies reveal that excipients, drug and both types of NP are haemcompatible and could be use for systemic administration.

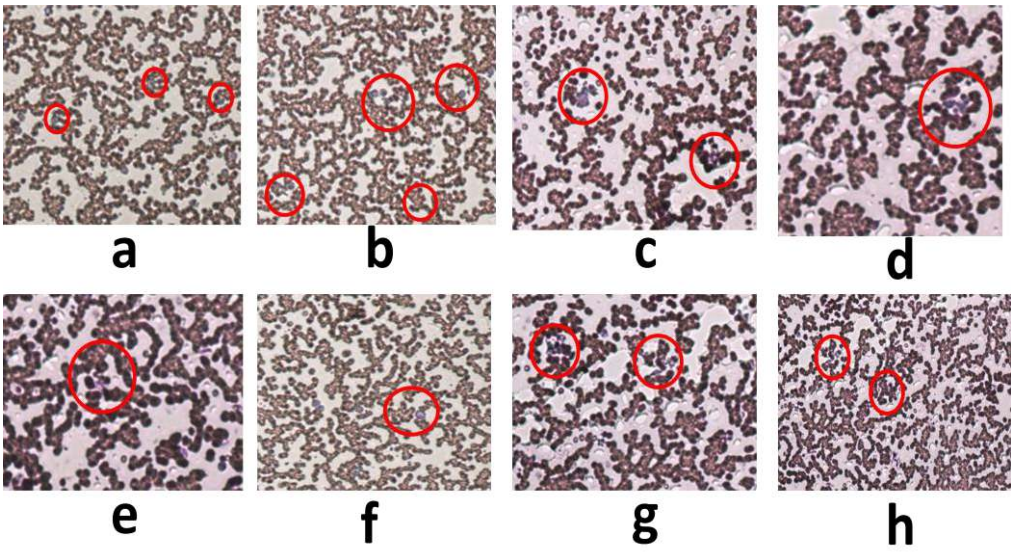

Figure 5.29. Platelet aggregation microscopic images of drug loaded BBR-NP, BBR-SCNP and placebos NP (45 x)

(a)BBR – NP (10 mcg/ml) (b) BBR – SCNP (10 mcg/ml) (c) BBR – SCNP (100 mcg/ml) (d) BBR – NP (100 mcg/ml) (e) BBR – Pure (10 mcg) (f) BBR – Pure (100 mcg) (g) BBR – NP Placebos (h) BBR – SCNP Placebos

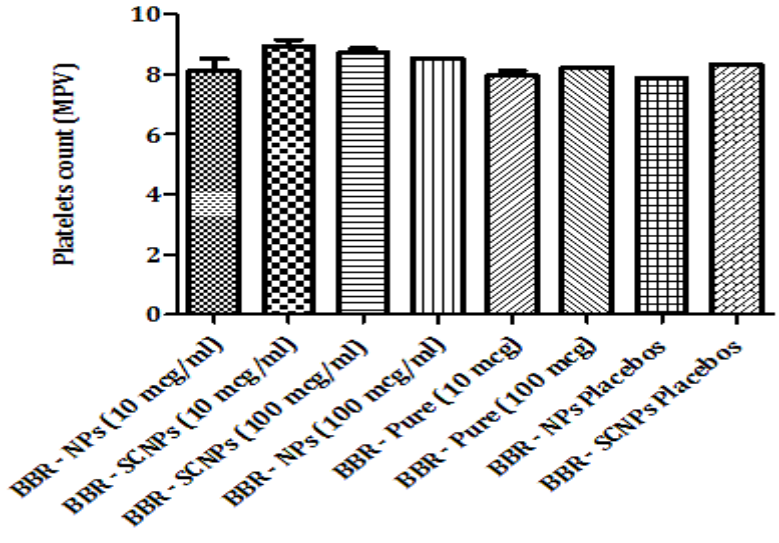

Figure 5.30. Platelet count results of BBR-NP, BBR-SCNP and placebos NP after incubation in blood

5.10. Toxicity study

Animals from second to fourth group did not show atypical behavioral changes compared to first group (control) during the study period. All groups of animals similarly received food and water without refuse. Serum AST, ALP and ALT levels of all groups were normal [Figure 5.31 (a, b & c)]. The serum urea and creatinine levels in all groups were also within normal range [Figure 5.32 (a) & (b)]. The normal values of Liver enzymes (AST, ALP and ALT) and Kidney enzymes (Urea and Creatinine) are tablulated in Table 5.15. It is confirmed that BBR, BBR nanoparticles or placebo NP does not induced liver or kindney toxicity and safe for long term consumption.

In histopathology analysis, undetectable abnormal lesions or cell disruption of intestine part of all groups compared to control group indicates there is no occurrence of mucosal irritation or damage after consumption of BBR at given dose as shown in Figure 5.33. Histopathology of liver sections of treated groups (II, III and IV) show normal hepatic architecture like prominent central vein and normal hepatocytes with stained nucleolus similar to control group. Stained liver sections confirmed that hepatic cell are with intact cell membrane and have no infiltration of inflammatory cells as depicted in Figure 5.34. Kidney sections of all group of animals show typical renal cell structures similar to control groups. The sections are show with normal renal cortex

with prominent glomerular tufts and absence of glomerular cell proliferation. There is no destroyed or ruptured tubular membrane in kidney of all groups which are depicted in figure 5.35. Appearance of normal cell structure of intestine, liver and kidney part of animals which were treated with BBR – SCNP and placebos confirmed non toxic nature of drug, excipients such as poly (ε) caprolactone (carrier) and vitamin E TPGS (p-gp inhibitor) in long term consumption.

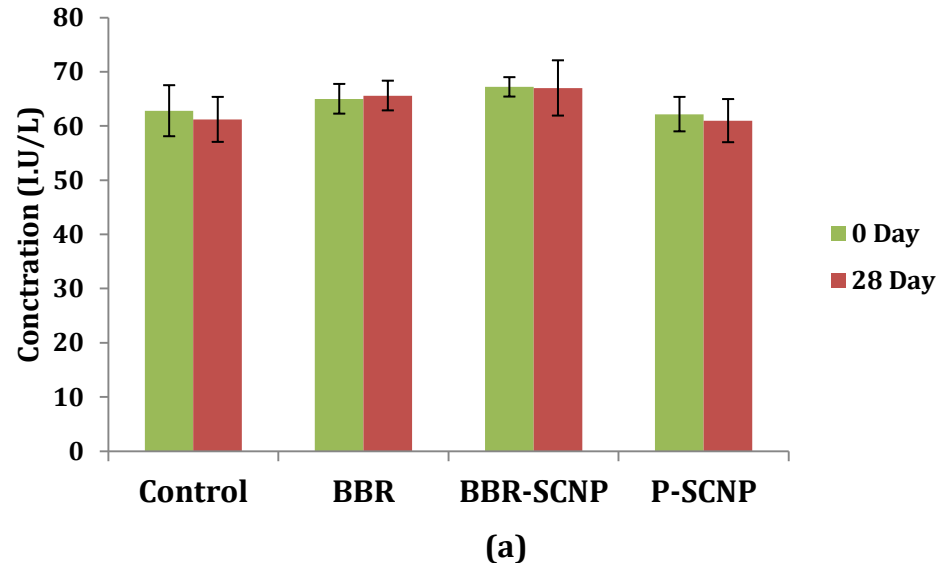

(a)

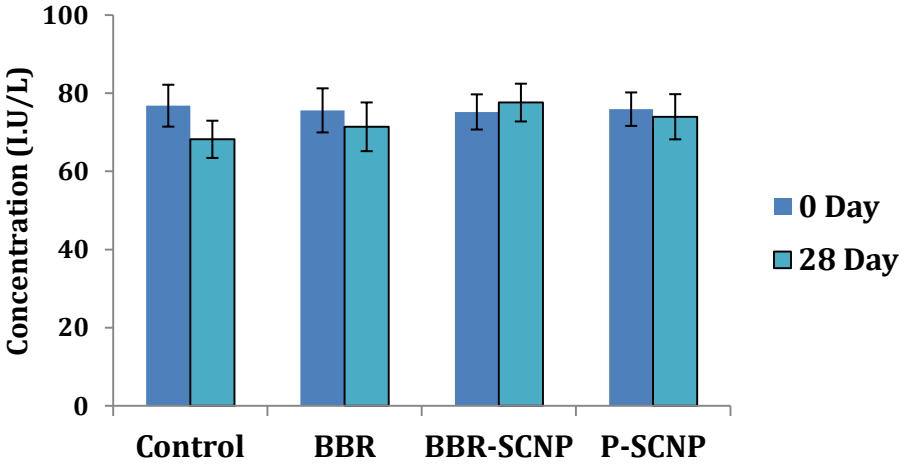

(b)

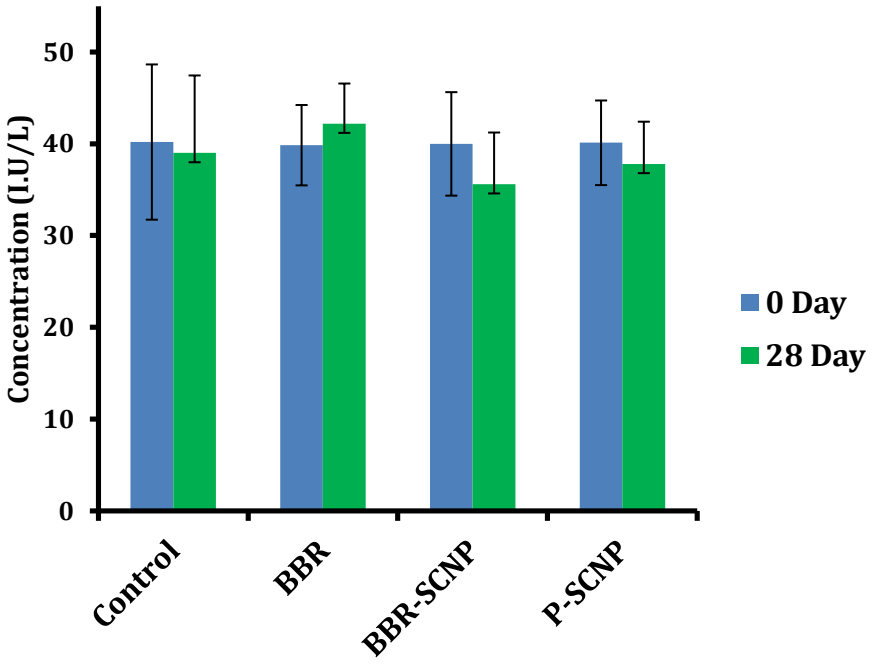

(c)

Figure 5.31. Quantification of different Liver enzymes (a) AST (b) ALP (c) ALT

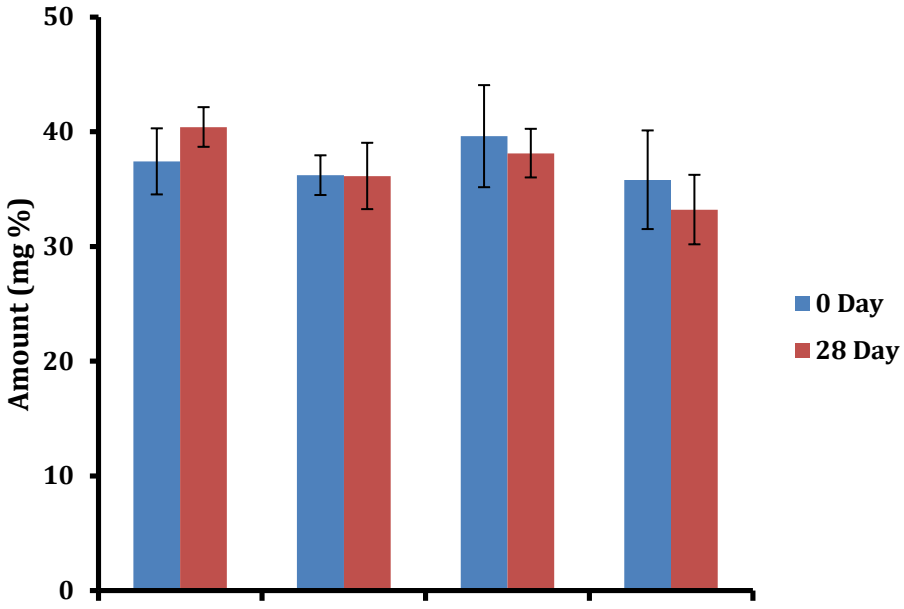

(a)

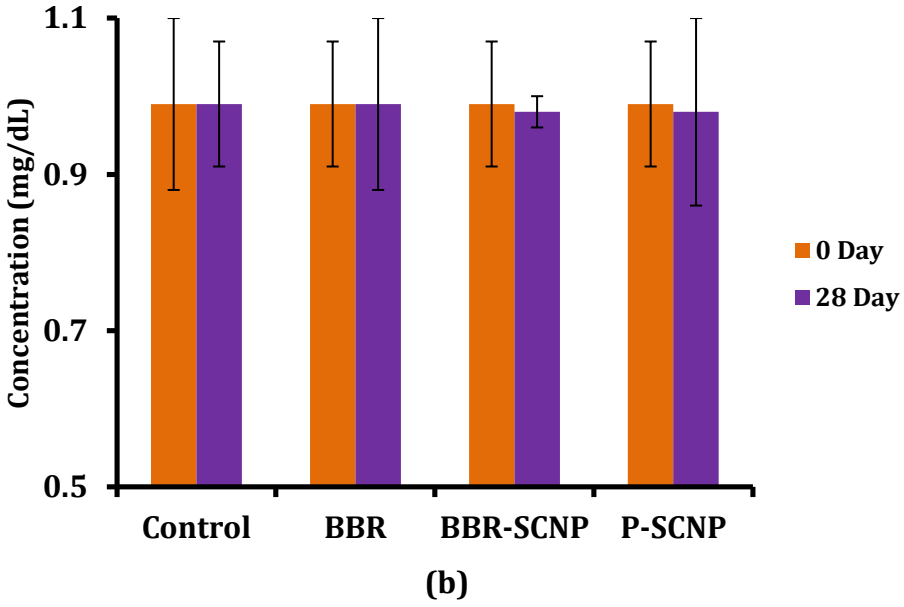

Figure 5.32. Quantification Kidney enzymes (a) Urea (b) Creatinine

Table 5.15. Liver and Kidney enzymes normal values

Organ	Enzyme	Normal values
Liver	AST	**45.7 – 80.8 (IU/L)**
	ALP	**56.8 – 128 (IU/L)**
	ALT	**22.3 – 68.6 (IU/L)**
Kidney	Urea	**20 – 50 mg %**
	Creatinine	**0.6 – 1.2 mg/dL**

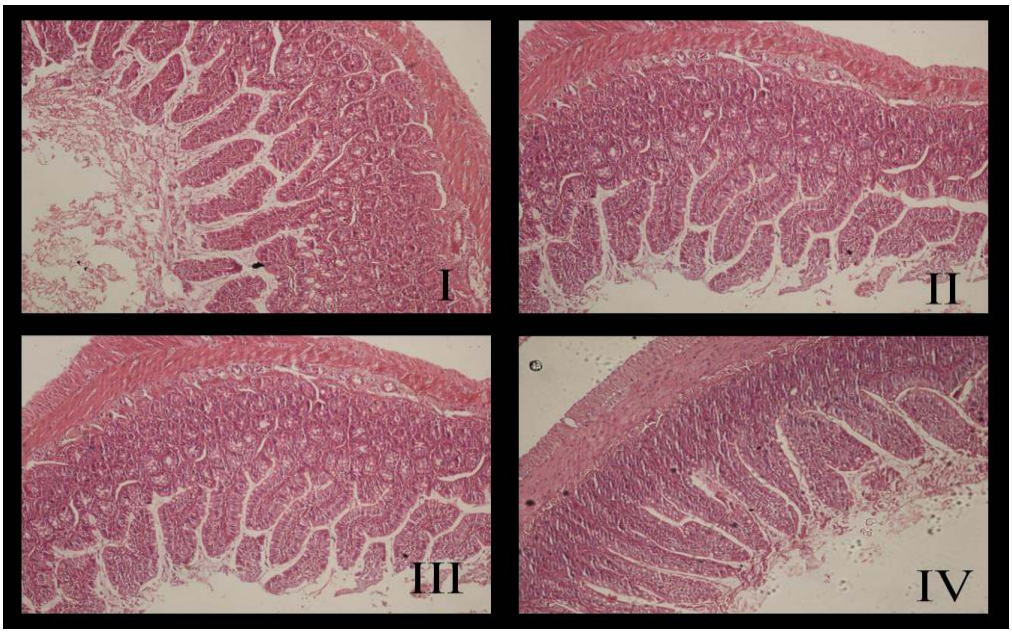

Figure 5.33. Microphotograph of intestine of different groups of animals

I. Control, II. BBR, III. BBR - SCNP and IV. Placebo - SCNP

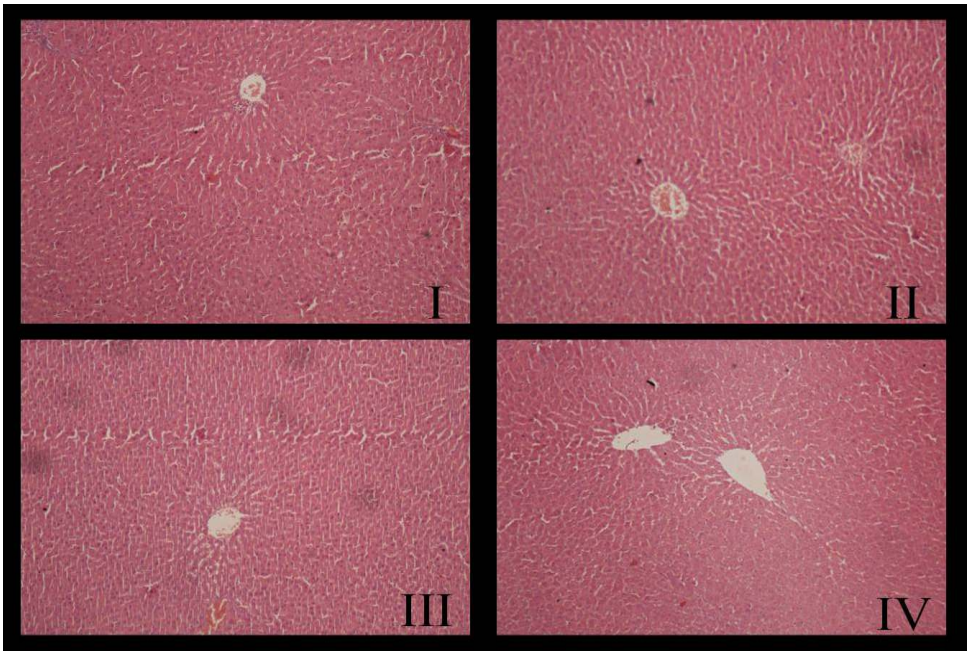

Figure 5.34. Microphotograph of liver of different groups of animals

I. Control, II. BBR, III. BBR - SCNP and IV. Placebo - SCNP

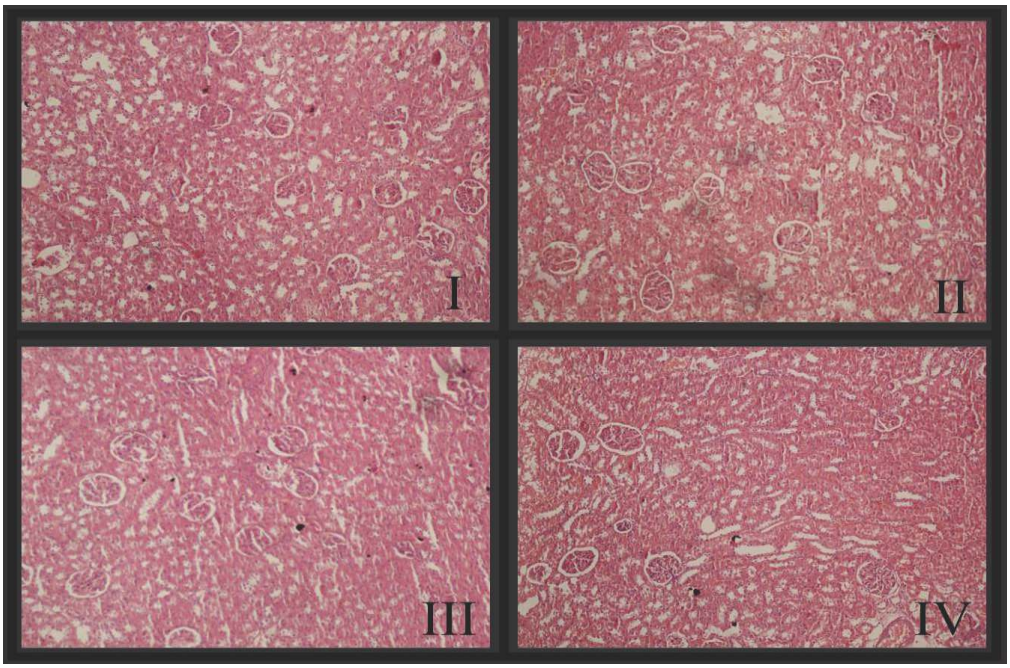

Figure 5.35. Microphotograph of kidney of different groups of animals

I. Control, II. BBR, III. BBR - SCNP and IV. Placebo - SCNP